ALCOA

# ALCOA RESEARCH LABORATORIES

ALUMINUM COMPANY OF AMERICA

ALUMINUM COMPANY OF AMERICA
Alcoa Research Laboratories
Chemical Metallurgy Division
New Kensington, Pennsylvania



# INVESTIGATION OF THE MECHANISM OF STRESS CORROSION OF ALUMINUM ALLOYS

Bureau of Naval Weapons Contract NOw 65-0327-f

Final Report

(Period of February 16, 1965, to February 16, 1966)

Reported by: J. McHardy
J. McHardy
Principal Research Engineer

Approved by: E. H. Hollingsworth
E. H. Hollingsworth
Project Supervisor

## Table of Contents

ALUMINUM COMPANY OF AMERICA
Alcoa Research Laboratories
Chemical Metallurgy Division
New Kensington, Pennsylvania

SYNOPSIS:

A basic investigation of the mechanism of stress-corrosion cracking in aluminum alloys of the 7075 family initiated under an earlier contract has been continued. As in the earlier contract, the main experimental technique involved the use of cathodic protection to control the corrosion of specimens in an aggressive electrolyte capable of producing stress corrosion failure rapidly.

The results suggest three stages in the stress corrosion process with the rate of penetration of corrosion or cracking increasing with each succeeding stage. In the first stage, stress corrosion takes place independently of stress, that is, it follows the same course as the general corrosion of an unstressed specimen; for the alloys investigated this general corrosion occurred as random pitting. In the second stage, the attack becomes intergranular (if not already of this type) and directional, and it leads to the development of cracks of a microscopic size, or larger; these are the "secondary" cracks frequently seen in specimens that fail by stress-corrosion cracking. The third stage initiates whenever one of the intergranular cracks developed in the second stage progresses far enough for the yield strength of the specimen to be reached; and it continues to the point of tensile failure.

Pits play an important role as stress risers for initiation of the second stage. The association of these pits with the first signs of intergranular attack is revealed in electron micrographs. And, at lower levels of cathodic protection, where the numerous pits formed by general corrosion are poor stress risers, stressed specimens have surprisingly long lives with the result that time-to-failure does not increase progressively with potential, but rather passes through a maximum.

The third stage appears to involve preferential dissolution of the tip of a crack resulting from strain induced anodic depolarization of locally yielding metal, as proposed by Hoar. Evidence for the occurrence of yielding is that the stage initiates at a stress independent of the initial load, and that 'yawning', or visible opening, of a crack occurs during this stage. Evidence for the electrochemical factor is the strong dependence of crack propagation rate upon potential. Some data indicate that the second and third stages are both prevented at the same potential - suggesting that they are related processes. One intriguing possibility is that yielding in the third stage is paralleled by creep in the second stage, as suggested for another system by Swann and Embury.

Iron, silicon and chromium do not have a large effect upon the electrochemical behavior of the phases in 7075 alloy, suggesting indirectly that any effect they may have upon stress corrosion performance is mostly the result of their effect upon precipitation.

INTRODUCTION:

This report summarizes an investigation of the mechanism of stress-corrosion cracking of aluminum alloys. The investigation, carried out at the Alcoa Research Laboratories under Bureau of Weapons Contract NOw 65-0327-f, was a continuation of an investigation under a previous contract, NOw 65-0170-c (1). The objective of the investigation was the same as that of the earlier one - to establish more firmly the premise that the stress corrosion of an aluminum alloy depends, not upon metallurgical structure alone, nor upon the electrochemical characteristics of this structure in a specific environment alone, but rather upon these two factors acting together. As the work progressed, three specific objectives became defined: (1) to develop a better picture of the electrochemical effect of stress, (2) to investigate the processes occurring during crack initiation and crack propagation, and (3) to identify the microstructural features associated with these two processes.

As in the earlier contract, experimental work centered around the cathodic protection of specimens in an aggressive electrolyte that produced stress corrosion of susceptible specimens rapidly. This protection was used to control corrosion and stress corrosion, and to establish the potential of the most anodic phase involved in corrosion or stress corrosion. (In theory, at least, corrosion or stress corrosion should stop whenever cathodic polarization equals or exceeds the potential

of the most anodic phase involved in these processes.) Attention was directed specifically toward establishing cathodic protection curves for various alloys in the 7075 family showing the relation of the time to failure of a susceptible, stressed specimen to the level of cathodic protection. Again, attention was given to the kinetics of stress corrosion by following the course of this corrosion under various levels of cathodic protection. And, finally, considerable attention was directed toward establishing the microstructural features associated with the stress corrosion process under the various experimental conditions used.

MATERIALS:

Plate - Specimen blanks (0.25 inch x 0.25 inch x 2 inches) were taken in the short transverse direction from the same production lot of 2-inch thick 7075-T651 alloy plate used for the previous contract. These blanks were reheat-treated, quenched in cold water and artificially aged to the -T6 and -T73 tempers. The chemical analysis of the plate and its tensile properties and electrical conductivities in the -T6 and -T73 tempers are listed in Tables I and II. The properties differ slightly from those reported in the previous contract because a new lot of specimen blanks was reheat-treated for the present contract, and the properties are affected slightly by such factors as small variations in quenching rate. The microstructure of the plate in the -T6 temper is illustrated in Figure 1.

Forgings - Four alloys were prepared to represent compositional variations of 7075 alloy. The alloys were cast as

9-inch diameter D.C. ingots, preheated 16 hours at 870°F, cut into sections 6 inches high and scalped to a diameter of 8.5 inches. One section was then forged into a bar 2 inches x 4 inches x approximately 40 inches long.

Five forgings were made from the four alloys; one alloy was forged at two temperatures. Throughout the report, the forgings are identified as follows:

1. Nominal 7075-T6 Alloy (S. No.* 321852). Forged at 650°F, the nominal forging temperature used for 7075 alloy in the Fabricating Laboratory.

2. Recrystallized 7075-T6 Alloy (S. No. 321853). Forged from a section of the same ingot used for (1) but at a lower temperature, 500°F, to insure that subsequent heat-treatment would produce recrystallization.

3. High Purity 7075-T6 Alloy (S. No. 321854). An alloy with small amounts of impurities (Fe, Si, Mn).

4. Nominal 7075-T6 - Cr Alloy (S. No. 321615). An alloy without added chromium.

5. High Purity 7075-T6 - Cr Alloy (S. No. 321780). An alloy with small amounts of impurities (Fe, Si, Mn) and without added chromium.

Conditions were selected to produce recrystallization during heat treatment in (2) but not in (1). No attempt was made to produce recrystallization in the other alloys, but it was anticipated in (4) and (5), the two alloys without chromium; however, x-ray analysis of heat treated and artificially aged specimens

---

*S. No. - Abbreviation for "Specimen Number."

(-T6) revealed that, in fact, all five forgings yielded fully recrystallized structures.

The chemical analysis of the four melts used for the five forgings are listed in Table I. Typical microstructures in the -T6 temper are illustrated in Figure 1. Tensile properties and electrical conductivities are listed in Table II.

All specimen blanks (0.25 inch x 0.25 inch x 2 inches) were taken in the short transverse direction from the center 2 inch portion of a forging and then solution heat treated, quenched in cold water and artificially aged immediately to the -T6 temper. Comparison of the microstructures of the five forgings with periods of heat treatment from 1 to 16 hours revealed that a 4 hour period dissolved substantially all soluble precipitate; and this period was used generally.

The uniformity of the center 2 inch portion of each forging was demonstrated by a survey of electrical conductivies and short transverse tensile properties across the width of -T6 temper transverse sections and also by examination of these sections after macro-etching. The maximum variation in tensile strength or yield strength of short transverse specimens from the center portion of any one forging did not exceed 5%.

## EXPERIMENTAL:

General - With only one addition - a new test specimen - the experimental conditions, techniques and solution were the same as in the preceding contract (1).

Cathodic Protection Experiments - The apparatus and circuits used for the cathodic protection experiments provided means for: (1) Potentiostatically controlling the potential of a specimen to within ± 0.5 mv, with a maximum drift because of variations in IR drop of less than 5 mv; (2) monitoring the continuity of a stressed specimen to provide a record of the time to failure; and (3) measuring the electrical resistance of a specimen during the test. All resistances were corrected to 20° C. The temperature coefficient of resistance ($\alpha$) was calculated from the empirical relationship developed at the Alcoa Research Laboratories:

$$\alpha = \frac{(\text{conductivity in \%IACS})}{61} \times 0.00403$$

Cathodic protection was applied to a specimen immersed in 9 liters of a solution containing: 1.00 mole/liter of sodium chloride, 0.21 mole/liter of aluminum chloride and maintained at a pH of 1 ± 0.05 by the addition of hydrochloric acid. Fresh solution was made up periodically to minimize the build-up of corrosion products. Contamination of the solution from the two aluminum anodes was minimized by isolating them in separate compartments, and by replacing the solution in the compartments every day.

Tensile Specimens - Standard 0.125 inch tensile specimens were machined from specimen blanks and stressed in electrically insulated "constant strain" fixtures. Electrical leads needed for resistance measurement and connection to the potentiostat were attached to a specimen by percussion welding. A Luggin

capillary was mounted through a hole drilled in the side of the stressing fixture with the tip 0.3 cm from the specimen. Correction for IR drop was relatively simple, since the potential distribution followed that for concentric cylinders for distance up to about 1 cm from a specimen. The calculation of the correction for IR drop is given in Appendix A.

Sheet Specimens - A new specimen was developed during the investigation to facilitate the direct examination of a corroded surface by electron microscopy. The miniature sheet specimen could be stressed by bending in a Plexiglass fixture as illustrated in Figure 2. It was prepared from the same blank used for a tensile specimen; up to three specimens were obtained from each short transverse 0.25 inch x 0.25 inch x 2 inch blank. A specimen was taken from a blank in such a way that its two larger faces were transverse sections through the original forging.

Each specimen was machined to dimensions of 2 inches long x 0.25 inch wide x 0.020 to 0.035 inches thick. It was then mounted in Lucite and one face was given a metallographic polish: this operation removed 0.005 to 0.010 inches of metal. The specimen was then cut out of the mount, its thickness measured in 10 locations along the length and an average thickness calculated. (The measurements were performed with a sheet of paper protecting the polished surface; the thickness of the paper was determined later and subtracted from the actual measurements.)

Stress was applied by bending, employing the relationships for bent beam specimens derived by Haaijer and Loginow (2). These authors published a series of graphs of $\frac{\sigma}{E}$ versus $\frac{L - H}{H}$ for various values of $\frac{H}{t}$. (Where $\sigma$ is the required surface stress - 55,500 psi* was used in all present tests; $E$ is Young's Modulus - $10.3 \times 10^6$ psi for 7075 and the related alloys; $L$ is the undeformed length of a specimen; $H$ is the deformed length, i.e. the size of the fixture - 1.75 inches was selected for these tests; and $t$ is the thickness of the specimen.)

In order to find the value of $L$ which would produce the required strain, it was first necessary to calculate $\frac{H}{t}$, i.e. to divide the thickness of the specimen into 1.75 inches. The ratio of $\frac{L - H}{H}$ was then read from the appropriate curve. In practice, it was usually necessary to interpolate between two of the published curves, since they applied only to discrete values of $\frac{H}{t}$.

Once the ratio $\frac{L - H}{H}$ had been found, a specimen was carefully filed down to the appropriate length, $L$, and then prepared for exposure. The preparation involved painting the specimen with "Micromask Lacquer" (electroplaters stop-off) to expose a polished area 0.25 inch x 1.24 inch (i.e. 2 square cm) and then carefully springing it into the Plexiglass fixture. Next, five electrical leads were attached to the specimen by percussion welding: four for resistance

---

* A stress of 55,500 psi was 75% of the yield strength of the 7075-T6 alloy plate. For the other products, this stress was a different percentage of the yield strength, but for the metallographic examination, the difference was not considered significant.

measurements** and one for connecting to the potentiostat. The leads passed through holes drilled for the purpose in the fixture. Finally, electroplaters' stop-off was applied to all the remaining areas of exposed metal (with the exception of the polished surface), and the exposure was started.

A Luggin capillary was placed 0.3 cm from the center of the specimen during the test; an empirical derivation of the IR correction for this situation is given in Appendix A.

After exposure, a specimen was removed from its fixture and rinsed in distilled water. Nitric acid was used to clean off the film of corrosion product, and the specimen was anodized in tataric acid to make an oxide replica of the corroded surface. (It was this procedure that necessitated the use of electroplater's stop off: the mixture of beeswax and rosin normally used for electrochemical tests would have ignited in contact with the perchloric acid used to remove the replica.)

Potential Measurements - All potential measurements were made against a saturated calomel reference electrode, using a Leeds and Northrup 8687 potentiometer.

The European sign convention in which the potential of an active metal has a negative sign is used throughout this report.

RESULTS:

Cathodic Protection Curves for the 7075 Family of Alloys - The effect of cathodic protection on the time to failure by stress-corrosion cracking for specimens in the -T6 temper from

---

** Unfortunately, bubble formation at the stop-off interface resulted in spurious corrosion which invalidated the resistance measurements, and these difficulties were not overcome.

the 7075 family of alloys is shown in Figures 3 - 6. All the curves are similar in form and differ only in relative position. As cathodic protection was increased, stress corrosion life first increased to a maximum, then decreased to a minimum - comparative with the free corrosion life - and finally rose again towards infinity.

The curve in Figure 3 differs from the cathodic protection curve which summarized the basic results of the first contract only by the presence of the rather surprising "hump" or the maximum at about -0.950 volts. As indicated by the two sets of points, the maximum could not have been predicted from the old data, and is based entirely on the new data. At first the maximum was regarded with some skepticism, but considerable work eventually left little question about its validity. It is interesting to note that some evidence of a maximum was found almost two years ago when preliminary work was in progress, but at that time, because the experimental techniques were not fully developed, the results were considered unreliable and were disregarded.

Alloying variations had two major effects on the cathodic protection curve. The maximum at lower levels of protection was less pronounced for the alloys free of chromium, and the potential required to prevent failure (the "Protection Potential") was more negative for the alloys with a high purity base. The latter effect was quite pronounced, and in fact, the protection potential was never actually attained for the high purity alloys.

The shape of the cathodic protection curves indicates that the protection potentials lie in the range of -1.400 to -1.500 volts, where cathodic corrosion occurs.

Kinetics of the Stress Corrosion Process: The Resistance - Time Curve - In the earlier contract, measurement of the electrical resistance of a specimen was originally proposed as only one of several techniques by which the course of stress corrosion could be investigated. However, it soon proved to be the most suitable technique considered. Specifically, the increase in the resistance of a specimen as a function of time provided a great deal of information about the kinetics of stress-corrosion cracking, and establishing the "Resistance-Time Curve" became the basic technique for this purpose.

Typical resistance-time curves are illustrated in Figures 7 - 11; the figures include data both from the present contract and from the previous one.

Analysis of resistance-time curves for stressed specimens leads to the conclusion that three consecutive stages are involved in the stress corrosion process: a first stage where the resistance-time curve coincides with the one for an unstressed specimen; a second stage, where the curve is roughly linear and pulls away gradually from the one for an unstressed specimen; and a third stage where the curve rises exponentially until the point of failure.

The duration of any one stage was strongly influenced by potential, and it was unusual for more than two of the stages to last long enough to show up clearly on a resistance-time

curve. One curve in which the three stages are all well defined is shown in Figure 8c, but the existance of three stages can also be deduced by analysis of the curves in Figures 7 - 11. The absence of evidence in a curve for any one stage does not imply, of course, that the stage was absent, but rather that it was too brief or too poorly defined to be detected.

At most potentials, the first stage was a poorly defined part of the resistance-time curve, the total resistance change being less than the experimental error of $\pm$ 0.1%. The most convincing evidence for the existance of the first stage was obtained with specimens exposed at -0.950 volts, as illustrated in Figure 7. A potential of -0.950 volts was unique in several ways; for one thing, it was close to the potential at which the maximum in the cathodic protection curve occurred. Some of the unique aspects of this potential are discussed later.

The apparent lack of any effect of stress upon the resistance-time curve leads to the conclusion that the first stage is identical with the corrosive attack that occurs in unstressed specimens.

The second stage was generally better defined than the first stage, but the total resistance change was still rather small, being only a little more than the experimental error. One curve in which the second stage is defined by more data points than usual is shown in Figure 9.

Visual examination of a specimen undergoing the second stage of stress corrosion indicated no difference in appearance

from that of an unstressed specimen. Except at free corrosion, the only visible change in either stressed or unstressed specimens was a gradual loss of reflectivity. Some penetration of a stressed specimen must occur in the second stage to account for the increase in resistance that is observed. One explanation, which is consistent with observations to be presented later, is that the penetration takes the form of intergranular cracks too small to be seen with the naked eye.

The exponential form of the third stage of the curve was established in the earlier contract. Examples of the third stage, plotted on semilogarithmic axes to emphasize the exponential increase in resistance with time, are given for two alloys in Figures 10 and 11. Inspection of the curves draws attention to two important features of the third stage, both of which were recognized in the earlier contract; (1) Figure 10 demonstrates that the slope of a curve is independent of initial stress and (2) Figure 11 demonstrates that the slope of a curve is influenced strongly by potential, becoming less as cathodic protection is increased.

As Figures 8 and 9 indicate, the duration of the third stage was usually quite short, and it was often missed completely, either because it all occurred overnight, or simply because it occurred so rapidly that it fell between scheduled resistance measurements. In general, several experiments had to be performed before a single complete curve was obtained.

Evidence cited in the earlier contract suggested that the on-set of the third stage corresponded to the point at which

the yield strength of a specimen was reached. The evidence was drawn from Figure 8, which indicates that initiation of the third stage required a greater depth of crack development during the preceding stage, the lower the initial stress. In fact, a roughly linear plot was obtained between the resistance change required to initiate the third stage and the calculated decrease in cross-sectional area required to reach the yield strength.

The deduction that may be drawn from this evidence, combined with the fact that the third stage is strongly dependent upon potential, is that the process occurring somehow involves an interaction between corrosion and mechanical yielding.

Consider now in greater detail the results at -0.950 volts. At the end of the earlier contract, resistance-time curves had been established for the 2 inch thick 7075-T6 alloy plate at three potentials: -0.750 volts (free corrosion), -1.150 volts and -1.290 volts. Almost immediately some rather surprising results were obtained when measurements were continued in the present contract. First, as already discussed, the time to failure was much longer than expected. Second, it became increasingly clear that the resistance-time curve for most of the life of a stressed specimen was coincident with the curve for an unstressed specimen, as shown in Figure 7.

The work pointed toward the conclusion that the rate of crack nucleation at -0.950 volts was relatively low while the rate of crack propagation was relatively high. To investigate this possibility further, specimens were pre-exposed at

-1.150 volts until an appreciable resistance change took place (indicating the development of one or more cracks) and then brought back to -0.950 volts. The results are summarized in Table III. With one exception, the life of a specimen at -0.950 volts was appreciably reduced by pre-exposure at -1.150 volts; in fact, the sum of the exposures at both potentials was less than that the normal life at -0.950 volts. In one instance, pre-exposure made possible enough measurements of the third (exponential) stage of a resistance-time curve to permit an approximate evaluation of the slope of this curve.

The effects of pretreatment at potentials other than -1.150 volts are summarized in Table IV. Somewhat surprisingly the results show that the life of a specimen at -0.950 volts may be reduced appreciably when pretreated for a long time at a protective potential. This result suggests that stress corrosion may proceed to some extent even at potentials where the overall process is prevented. Possible implications of this observation are discussed later.

In the earlier contract, the first stage of the resistance-time curve was not identified, and the results where discussed in terms of the last two stages only.

Metallographic Examination (Light Microscope) - Specimens that failed by stress-corrosion cracking at various potentials were sectioned and examined by light microscopy. Micrographs of selected specimens from the five forgings are shown in Figures 12 - 16. Similar micrographs of specimens from the plate were presented in the report of the previous contract.

Attention is called to four features of these micrographs:

1. All the specimens suffered pitting attack under conditions of free corrosion, somewhat surprisingly perhaps in view of the fact that the two chromium-free alloys are subject to intergranular attack in more conventional exposures. Undoubtedly, the pitting attack reflects the highly aggressive nature of the test solution used.

2. Relatively little cathodic protection was required to diminish the depth of pitting to a point where it was virtually invisible at 100X magnification. In no case can pits be seen clearly in a specimen exposed at -0.950 volts.

3. Confirmation of the view that the second stage of stress corrosion might involve the formation of intergranular cracks is evident, at least indirectly, from the micrographs. In almost all the specimens, the so-called "secondary cracks" frequently associated with a stress corrosion failure are observed. At free corrosion, the cracks all appear to originate from corrosion pits.

4. The number of secondary cracks was a minimum for each alloy in the specimen tested at -0.950 volts. It is clear, therefore, that the cracks were always slowest to develop at this potential. Taken in conjunction with the form of resistance-time curves obtained at -0.950 volts, the observation provides further evidence that the second stage of stress-corrosion cracking is the development of intergranular cracks.

Metallographic Examination (Electron Microscope) - The major part of the electron microscopic examination was devoted to comparing the effects of cathodic protection on four series of pre-polished specimens from the 2 inch plate. The four series represented unstressed and stressed specimens of both the -T6 and -T73 tempers. The results appear in Figures 17 - 36. Figures 37 and 38 are electron micrographs of specimens from the high purity 7075-T6 alloy forging.

Although not apparent from the micrographs alone, there was an effect of cathodic protection on the frequency of pitting in the unstressed -T6 temper specimens from the plate. As protection was increased, the number of pits decreased. The trend was fairly gradual, all the way from free corrosion (many pits) to the protection potential (almost no pits). The effect is in marked contrast to the very rapid effect of cathodic protection on the depth of pitting observed in the light micrographs.

Stressed -T6 temper specimens from the plate exposed at -0.750 volts (Figure 22) and -0.950 volts (Figure 23) appeared very similar to the corresponding unstressed specimens (Figures 17 and 18). The fact that no cracking developed during the exposures provides good evidence that the first stage of stress-corrosion cracking is identical with the corrosion attack on unstressed specimens, and in this system at least takes the form of random pitting.

Indications of the first signs of intergranular attack are apparent in the stressed -T6 temper specimens from the

plate exposed at -1.150 volts and -1.250 volts (Figures 24 - 26). In each case, the intergranular attack was associated with a corrosion pit. This observation, of course, suggests that pits formed during the first stage play an important role in the initiation of the second stage. Furthermore, since stress is apparently necessary for the development of intergranular attack (at least in the present series of 7075-T6 alloy specimens), the significant function of a pit is probably that of a stress riser. Constituent particles were also associated with the intergranular attack in most cases, and they, too, probably served to concentrate the stress; they may also have contributed to the attack galvanically.

An intergranular crack is evident in a stressed -T6 temper specimen from the plate exposed at -1.350 volts (Figure 27); this anomaly is discussed later.

The electron micrographs of -T73 temper specimens from the plate confirm the superior resistance to stress-corrosion cracking of this temper. Pitting was the only type of attack observed in the specimens, and there was no apparent effect of stress. Cubic (crystallographic) type pitting was more highly developed than in -T6 specimens, but the incidence of cubic pits bore no apparent relationship either to stress or to potential.

The "pebbled" appearance of the stressed -T6 specimens from the high purity 7075 alloy forging (Figures 37 and 38) may reflect damage to the surface during the rather long

exposures (possibly by hydrogen bubbles streaming upwards). The effect became more pronounced with the length of an exposure and after four days it completely obliterated every other feature of the surface. The micrographs provide two more examples of the association of a corrosion pit with intergranular attack, and further, they show that the initiation of intergranular attack may not require the presence of constituent particles, since none is visible in the micrographs.

Physical Significance of Resistance Change - Resistance has been used extensively to follow the course of corrosion and stress corrosion, but by itself, resistance yields only qualitative results. Two series of measurements were performed on tensile specimens in the -T6 temper from 7075 alloy plate to provide a better physical picture of the processes occurring during stress-corrosion cracking. In the first and more informative series, a correlation was obtained between the depth of a crack and resistance change (Figure 39). In the second series, a correlation was obtained between loss in tensile strength and resistance change (Figure 40).

Data for the correlation between crack depth and resistance change shown in Figure 39 were taken from specimens exposed at a variety of potentials and stress levels. The correlation is based upon two assumptions: (1) that the "bright" area on the fracture surface of a tensile specimen represented the full extent of the main stress corrosion crack immediately prior to mechanical failure, and (2) the resistance change obtained by extrapolating the resistance-time curve to the time of

failure was the full change associated with the main crack immediately prior to mechanical failure.

The first assumption is probably justified, since electron microscopic examinations of fracture surfaces have demonstrated conclusively that the "bright" area is intergranular in nature, and that the remaining area is not.

The second assumption is at best only approximately correct. On the one hand, there are generally a number of "secondary" cracks (except at potentials close to the maximum in the cathodic protection curve) which would make some contribution to the resistance change. On the other hand, at the potentials of lower cathodic protection, it is probable that extrapolation of the resistance-time curve underestimates the total resistance change since the "exponential" part of the curve is so short that it is usually missed.

The results in Figure 39 indicate a linear relationship between crack depth and the logarithm of resistance change. The deviation of the experimental points from the line of best fit is fairly consistent with the effects of the two factors mentioned above. The results imply that crack depth can be substituted for log $\Delta R$ in the third stage of a resistance-time curve; in other words, crack depth increases at a constant rate during this stage.

The relationship between loss in tensile strength and resistance change shown in Figure 40 provides an idea of the significance of a given change in resistance, and also tends to confirm microscopic observations (a) that more pits form at free corrosion

than at -1.150 volts and (b) that cracks develop only in stressed specimens. These conclusions follow from Figure 40 because the slope of a curve of tensile loss vs resistance change would increase with the "sharpness" of the sites of attack (e.g. cracks would be "sharper" than pits) and decrease with the number of sites of attack.

DISCUSSION:

The results of the investigation are gradually bringing into focus an overall picture of the stress-corrosion cracking of aluminum alloys (as represented by the behavior of 7075 alloy in an aggressive acid chloride solution). They point to three consecutive stages, with the rate of penetration increasing with each successive stage. The first stage occurs independently of applied stress; in the alloys used, it consisted entirely of random pitting. The second stage is stress dependent, and involves the development of small intergranular cracks. The third stage initiates whenever one of the intergranular cracks progresses far enough for the yield strength to be reached, and involves propagation of the crack until tensile failure occurs.

Other workers have recognized the first stage of stress-corrosion cracking in several systems. For example, Gruhl (3) demonstrated that the failure time of a specimen could be reduced by a pre-exposure unstressed, but only up to a certain point. In the present context, this point should correspond to the start of the second stage, i.e., to the initiation of intergranular cracks.

The vital role of stress in initiating the second stage is also substantiated by the work of Gruhl which shows that the first stage lasts longer the lower the applied stress. Considerable evidence in the present investigation - notably the association of corrosion pits with the first sign of intergranular attack - leads to the conclusion that the important function of a pit is to concentrate the applied stress. The duration of the first stage must then be governed by the time needed for a pit to form and create a threshold stress concentration in the vicinity of a grain boundary. The maximum observed in a cathodic protection curve implies simply a minimum in the stress concentration achieved by a pit at this potential. The results of metallographic examinations are consistent with this deduction. They show a progressive reduction in pit depth over the range of cathodic protection from free corrosion to -0.950 volts - an effect which would reduce the stress rising ability of a pit - and then, as protection is increased further, a gradual reduction in pitting frequency - an effect which would increase the share of the applied load for each pit, hence producing a greater stress concentration, and initiating the second stage sooner. The important effect of pitting on failure time resulting from its action as a stress riser was recognized by Mears, Brown and Dix more than 20 years ago (4).

Constitutent particles in a grain boundary also appear to act as stress risers, but they may not be essential for the development of intergranular attack.

Parkins (5) observed that the first sign of a visible crack coincides with the initiation of the final stage of stress-corrosion cracking in mild steels. He referred to the process as "yawning" of the crack, and demonstrated that it starts whenever the yield strength is reached. The main crack frequently has been detected visually during the third stage of stress corrosion in the present investigation - especially at the more negative potentials - but exactly when the "yawning" process begins has not been established.

Localized yielding would soon cease if it was the only process involved. The marked dependence of crack propagation rate upon potential leaves little question that corrosion is also involved; and hence that crack propagation occurs by the combined action of yielding and corrosion. A rough calculation (in Appendix B) yields a crack propagation rate of 0.05 inches/hour for a specimen of 7075-T6 at -0.950 volts. Interestingly, this value lies within the range of 0.02 to 0.08 inches/hour measured by Hoar and Hines for transgranular stress corrosion in stainless steels (6). To account for this rate purely on the basis of electrochemical dissolution, an anodic current density of about 1 ampere/square centimeter would be required (Appendix C): a current that is several orders of magnitude greater than corrosion currents normally encountered for aluminum.

Clearly, then, the role of yielding must be to enhance the corrosion rate. Two possible mechanisms whereby this

could occur have been proposed. One involves simple rupture of the protective oxide film, and the other - proposed by Hoar to explain transgranular stress-corrosion cracking of stainless steel - involves depolarization associated with the energy of dislocations emerging at the crack tip. The film rupture theory is difficult to reconcile with the results of the present investigation since the potential of unfilmed aluminum would be of the order of -2.000 volts which is considerably more negative than the protective potentials observed. Hoar's theory of strain induced anodic depolarization seems much more tenable.

The question arises: what is the significance of a protection potential? The electron micrographs suggest that pitting - the first stage of stress corrosion - is not prevented; the reduction in failure time at -0.950 volts produced by a long pretreatment under "complete" cathodic protection tends to confirm this view.

The second stage of a resistance-time curve has not been observed for any specimen held at a protection potential. It follows that crack initiation is the process that is prevented*, but on this information alone, nothing can be said about the third stage of the process, since it could not occur at all if the second stage did not preceed it. There is evidence, however,

---

* The micrograph in Figure 27 apparently contradicts this statement, and in fact, was once cited as evidence that crack initiation was not prevented. Until the micrograph is substantiated, however, the above statement appears to be the more rational interpretation of the overall results.

that the same potential would actually prevent both the second and third stages. A plot of crack propagation rate (in terms of $\frac{d(\log \Delta R)}{dt}$ - the slope of the third stage of a resistance-time curve) against potential is shown for two alloys in Figure 39. The curves apparently extrapolate to zero rate at potentials which are the same as the protection potentials for the respective alloys.

(Unsuccessful attempts in the previous contract to cathodically protect specimens once crack propagation had started must be considered inconclusive because of the possible failure of the whole protection current to reach the tip of the crack resulting from an IR drop in the crack. Evidence that appreciable IR drops may develop is shown in Figure 11: the increase in crack propagation rate in the last few hours of the life of the specimen exposed at -1.325 volts may well have resulted from an IR drop in the crack.)

Accepting the view that the second and third stages of stress-corrosion cracking are prevented at the same potential leads to the conclusion that they are closely related processes. Since the third stage apparently involves an interaction between corrosion and yielding, the interesting possibility arises that the second stage might involve an interaction between corrosion and creep. The idea has been proposed by other workers - notably Swann and Embury (7) who invoke a creep mechanism to account of the initiation of transgranular stress corrosion cracks in stainless steel.

The picture of stress-corrosion cracking described is based largely on data for 7075-T6 alloy, but it is supported by the more limited data for other alloys in the 7075 family. The data for these other alloys confirm expectations that there would be relatively small effects of compositional variations upon the electrochemical behavior of the phases in 7075 alloy. The evidence points more to the view that practical effects of alloying additions - notably the beneficial effect of chromium - result from variations produced in precipitation, for example, in the distribution of precipitate.

In summary, the investigation suggests three consecutive stages in the stress corrosion process. The mechanism of each stage has been elucidated to some extent, but many questions remain unanswered, especially about the second stage, in which intergranular cracks are formed. The stage may involve a process of creep, and this possibility should prove worthy of further investigation. Expansion of the investigation to include other alloy systems should also prove fruitful. Some work during this contract was actually started on the 2024 alloy family, but the acid chloride solution proved an unsuitable test medium, and a satisfactory solution was not found.

kad

REFERENCES:

(1) G. C. English, Bureau of Naval Weapons Contract NOw 64-0170-c. Final Report (Period of December 6, 1963, to February 6, 1965).

(2) G. Haaijer and A. W. Loginow, Corrosion 21, (4), 105-112, (1965).

(3) Wolfgang Gruhl, Z. Metallkde. 54, (2), 86-91, (1963).

(4) R. B. Mears, R. H. Brown and E. H. Dix, Symposium on Stress-Corrosion Cracking, (1945), 323-339.

(5) R. N. Parkins, "Some Aspects of the Influence of Deformation and Structure on Stress-Corrosion Cracking of Mild Steels" - a lecture delivered at U. S. Steel Research Center; Monroeville, Pennsylvania, on March 30, 1966.

(6) T. P. Hoar and J. M. West, Nature 187, (4612), 835, (1958).

(7) P. R. Swann and J. D. Embury, Second Berkley International Materials Conference on High Strength Materials, 327, (1964), John Wiley.

TABLE I

CHEMICAL ANALYSES

| S. No. | Alloy | % Cu | % Fe | % Si | % Mg | % Mn | % Zn | % Cr | % Ti |
|---|---|---|---|---|---|---|---|---|---|
| | **2-Inch Thick Plate** | | | | | | | | |
| 320831<br>311754 | 7075-T6<br>7075-T73 | 1.62 | 0.20 | 0.09 | 2.63 | 0.04 | 5.92 | 0.17 | 0.02 |
| | **2 Inch x 4 Inch Forgings** | | | | | | | | |
| 321852<br>321853 | Nominal 7075-T6<br>Recrystallized 7075-T6 (1) | 1.69 | 0.10 | 0.12 | 2.51 | 0.04 | 5.78 | 0.21 | 0.04 |
| 321854 | High Purity 7075-T6 | 1.77 | 0.00 | 0.01 | 2.57 | 0.00 | 5.85 | 0.24 | 0.04 |
| 321615 | Nominal 7075-T6 - Cr | 1.59 | 0.14 | 0.07 | 2.39 | 0.01 | 5.65 | 0.00 | 0.03 |
| 321780 | High Purity 7075-T6 - Cr | 1.55 | 0.00 | 0.02 | 2.52 | 0.01 | 5.60 | 0.00 | 0.03 |

Note: (1) Forged at low temperature to insure recrystallization during heat-treatment. In actual fact, all five forgings recrystallized.

TABLE II

CONDUCTIVITIES AND SHORT TRANSVERSE TENSILE PROPERTIES

| S. No. | Alloy | T.S. psi | Y.S. psi | Elongation % in 0.5 Inch | Conductivity % IACS |
|---|---|---|---|---|---|
| | | 2 Inch Thick Plate | | | |
| 320831 | 7075-T6 | 80,900 | 73,800 | 2.0 | 31.0 |
| 311754 | 7075-T73 | 71,550 | 67,400 | 3.0 | 38.5 |
| | | 2 Inch x 4 Inch Forgings | | | |
| 321852 | Nominal 7075-T6 | 81,350 | 71,620 | 9.5 | 32.2 |
| 321853 | Recrystallized 7075-T6 (1) | 81,600 | 71,380 | 10.0 | 31.9 |
| 321854 | High Purity 7075-T6 | 81,520 | 72,080 | 11.0 | 32.4 |
| 321615 | Nominal 7075-T6 - Cr | 73,350 | 63,580 | 12.0 | 32.9 |
| 321780 | High Purity 7075-T6 - Cr | 70,600 | 60,900 | 15.5 | 33.3 |

Note: (1) Forged at a low temperature to insure recrystallization during heat treatment. In actual fact, all five forgings recrystallized.

TABLE III

EFFECT OF PRETREATMENT AT -1.150 VOLTS ON TIME TO FAILURE AT -0.950 VOLTS OF 7075-T6 ALLOY SPECIMENS

| S. No. | Pretreatment - Hours | Time to Failure at -0.950 Volts - Hours | Total Life - Hours |
|---|---|---|---|
| 320831-N22 | None | 14.9 | 14.9 |
| 320831-N25 | None | 24.0 | 24.0 |
| 320831-N26 | None | 35.9 | 35.9 |
| 320831-N27 | 0.7 | 3.0 | 3.7 |
| 320831-N30 | 1.0 | 3.0 | 4.0 |
| 321831-N62 | 4.5 | 0.3 | 4.8 |
| 321831-N35 | 1.0 | 11.4 | 12.4 |
| 320831-N33 | 1.5 | 51.3 | 52.8 |

Note: Specimens from 2 inch plate stressed 75%Y.S.

TABLE IV

EFFECT OF PRETREATMENT AT PROTECTIVE POTENTIALS ON TIME TO FAILURE AT -0.950 VOLTS OF 7075-T6 ALLOY SPECIMENS

| S. No. | Alloy | Pretreatment Potential (Volts) | Pretreatment Time (Hours) | Time to Failure at -0.950 Volts (Hours) |
|---|---|---|---|---|
| | **2 Inch Thick Plate** | | | |
| 320831-N32 | 7075-T6 | -1.320 | 1.0 | 22.9 |
| | **2 Inch x 4 Inch Forgings** | | | |
| 321852-N5 | Nominal 7075-T6 | (No Pretreatment) | | 83.8 |
| 321852-N4 | Nominal 7075-T6 | -1.325 | 312.0 | 29.8 |
| 321853-N4 | Recrystallized 7075-T6 (1) | (No Pretreatment) | | 43.0 |
| 321853-N14 | Recrystallized 7075-T6 (1) | -1.375 | 299.0 | 28.6 |
| 321615-N15 | Nominal 7075-T6 - Cr | (No Pretreatment) | | 23.1 |
| 321615-N16 | Nominal 7075-T6 - Cr | (No Pretreatment) | | 21.8 |
| 321615-N28 | Nominal 7075-T6 - Cr | -1.325 | 289.0 | 5.2 |

Notes: (1) Forged at a low temperature to insure recrystallization during heat treatment. In actual fact, all three forgings recrystallized.

(2) Specimens stressed 75%Y.S.

Figure 1

Typical microstructures of longitudinal sections. For the plate, the section was taken from the center, halfway between the two surfaces; and for the forgings, the sections were taken from the center, halfway between the two edges as well as halfway between the two surfaces.

Etch: Keller's Mag: 100X

A. 7075-T6 alloy plate.
B. Nominal 7075-T6 alloy forging.
C. Recrystallized 7075-T6 alloy forging.
D. High purity 7075-T6 alloy forging.
E. Nominal 7075-T6 - Cr alloy forging.
F. High purity 7075-T6 - Cr alloy forging.

(The fabrication procedures were selected to yield recrystallization in (C) but not in (B). Actually, both forgings recrystallized during solution heat treatment.)

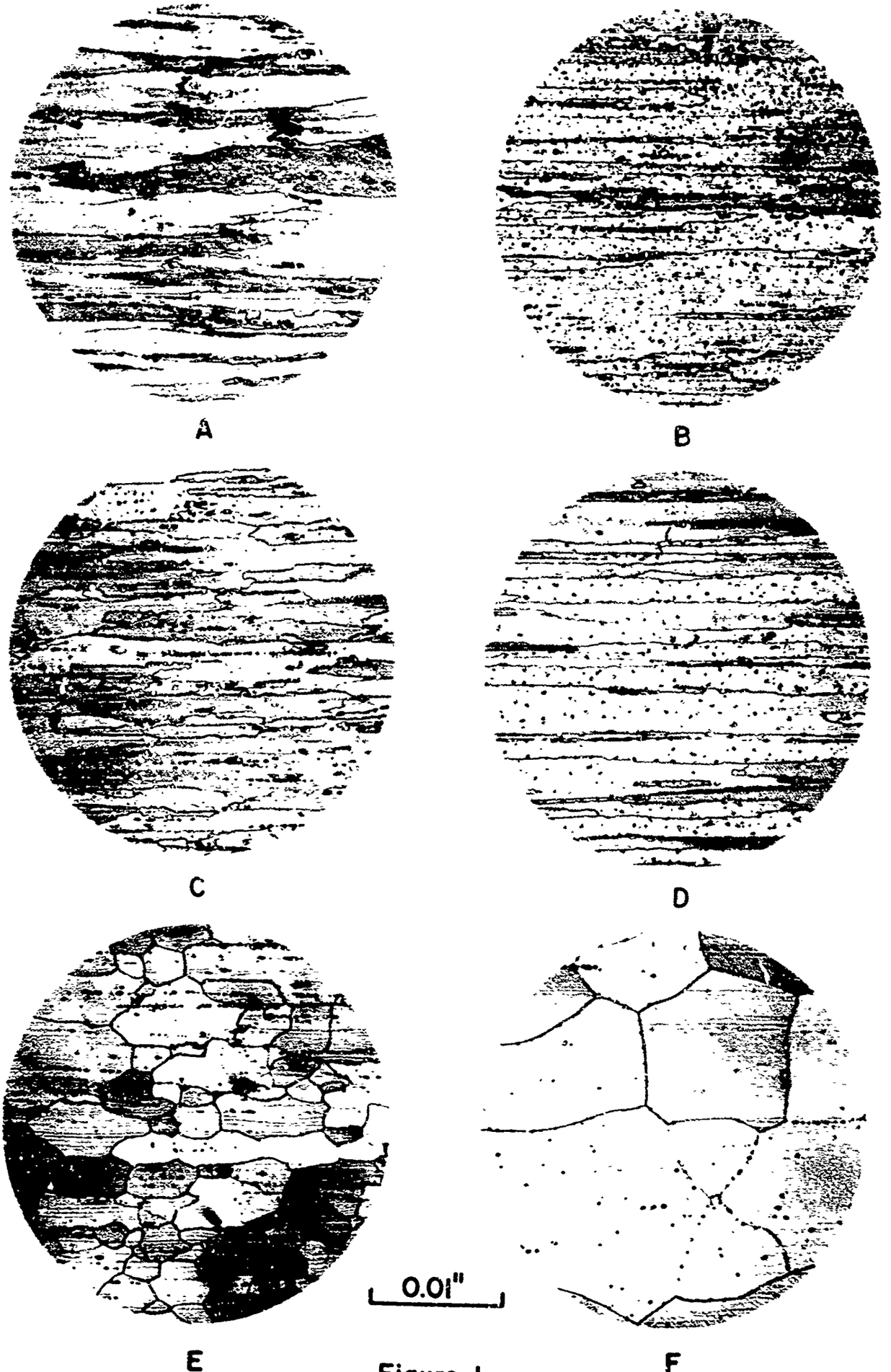


Figure 1

Figure 2

Pre-polished sheet specimen used for electron microscopic examination of a corroded surface. The specimen is masked off to expose 2 square centimeters and stressed by bending in the Plexiglass fixture. Electrical leads are attached to the specimen through holes in the fixture.

PEC010J

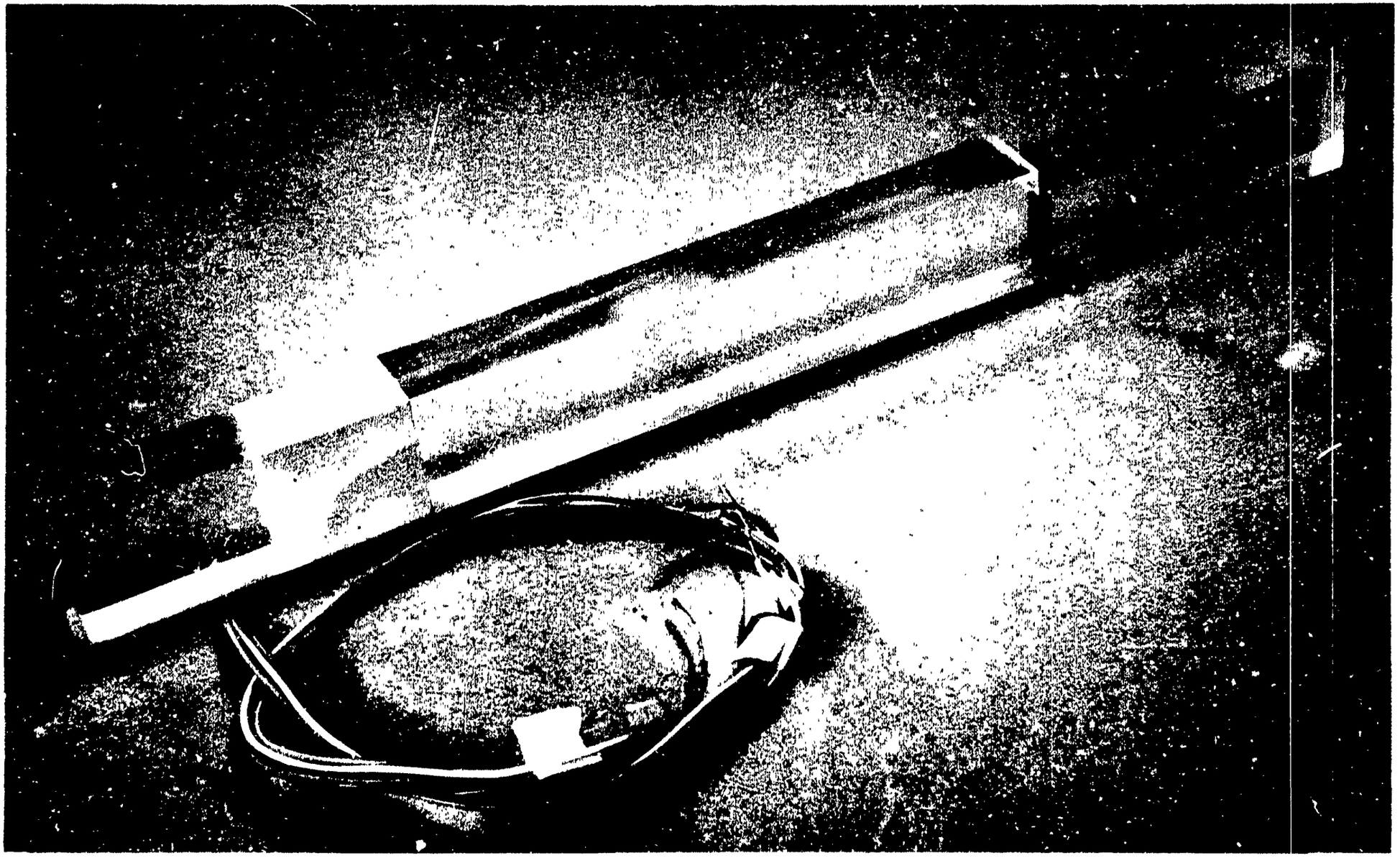

Figure 2

Figure 3

Cathodic protection curve for 7075-T6 alloy specimens from the short-transverse direction of 2 inch thick plate. Specimens were stressed in "constant strain" fixtures to 75% of the yield strength and exposed to the standard acidified chloride solution (as were all the specimens in Figures 4, 5 and 6). An open symbol means that the specimen did not fail.

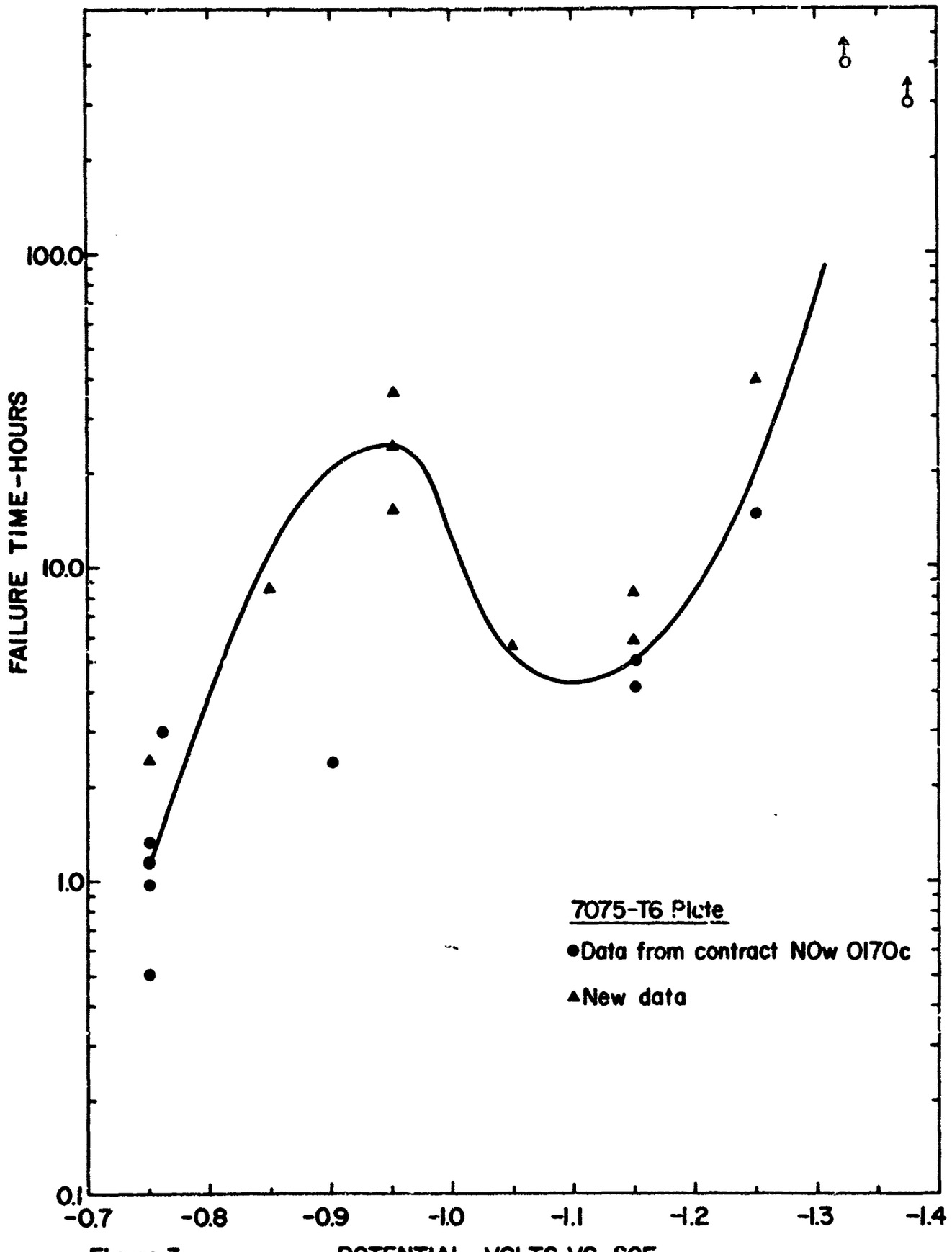
100.0
10.0
1.0
0.1
FAILURE TIME-HOURS
-0.7
-0.8
-0.9
-1.0
-1.1
-1.2
-1.3
-1.4
POTENTIAL-VOLTS VS. SCE
7075-T6 Plate
●Data from contract NOw 0170c
▲New data

Figure 3

Figure 4

Cathodic protection curve for 7075-T6 alloy specimens from the short-transverse direction of 2 x 4 inch forged bars. The "recrystallized" specimens were taken from a bar forged at a lower-than-normal-temperature to insure that recrystallization would occur during subsequent heat-treatment. X-ray analysis indicated later that both lots of specimens were in fact fully recrystallized (as were the specimens in Figures 5 and 6). An open symbol means that the specimen did not fail.

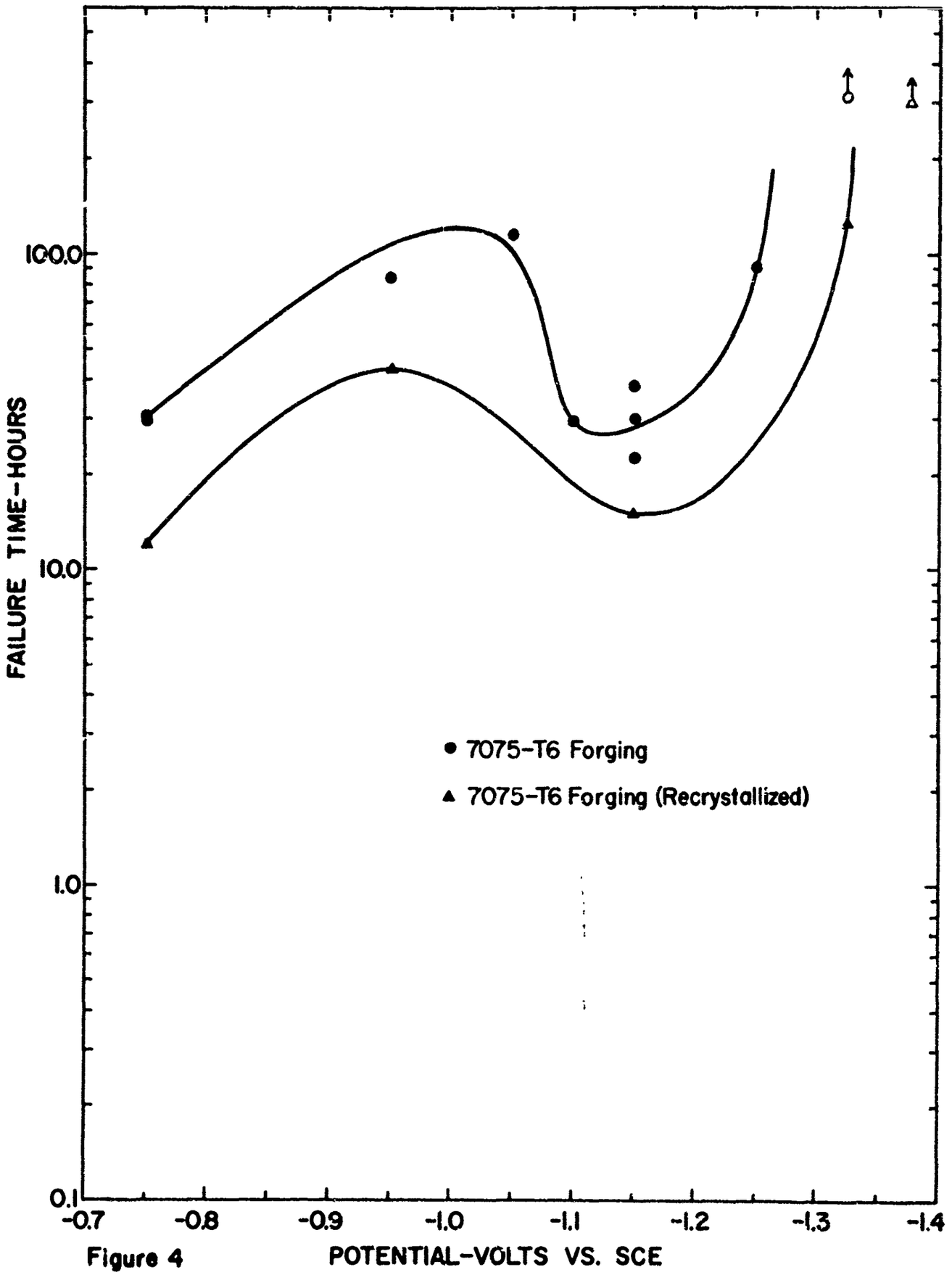
100.0
10.0
1.0
0.1
FAILURE TIME-HOURS
-0.7
-0.8
-0.9
-1.0
-1.1
-1.2
-1.3
-1.4
POTENTIAL-VOLTS VS. SCE
● 7075-T6 Forging
▲ 7075-T6 Forging (Recrystallized)

Figure 4

Figure 5

Cathodic protection curve for high purity 7075-T6 alloy specimens from the short-transverse direction of a 2 x 4 inch forged bar. Note that all specimens eventually failed: the shape of the curve implies that a potential of -1.400 or more negative would have been required for complete protection, and this potential is in the range where cathodic corrosion occurred.

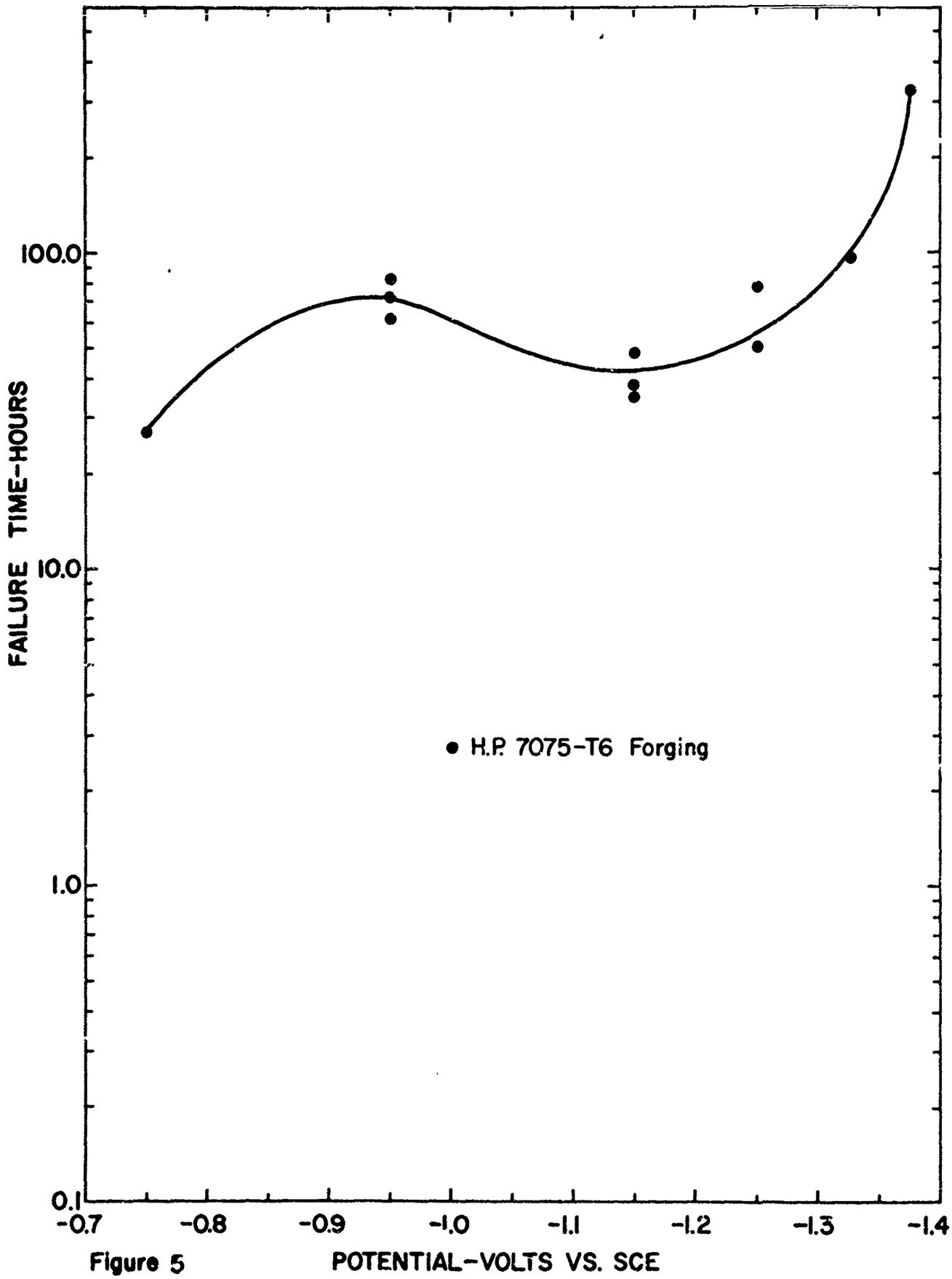
100.0
10.0
1.0
0.1
FAILURE TIME-HOURS
● H.P. 7075-T6 Forging
-0.7
-0.8
-0.9
-1.0
-1.1
-1.2
-1.3
-1.4
POTENTIAL-VOLTS VS. SCE

Figure 5

Figure 6

Cathodic protection curves for chromium free specimens of high purity and nominal purity 7075-T6 alloy taken from the short-transverse direction of 2 x 4 inch forged bars. The open symbol means that the specimen did not fail. Note that the high purity specimens all eventually failed. The shape of the curve implies that a potential somewhat more negative than -1.400 volts would have been required for complete protection, and this potential is in the range where cathodic corrosion occurred.

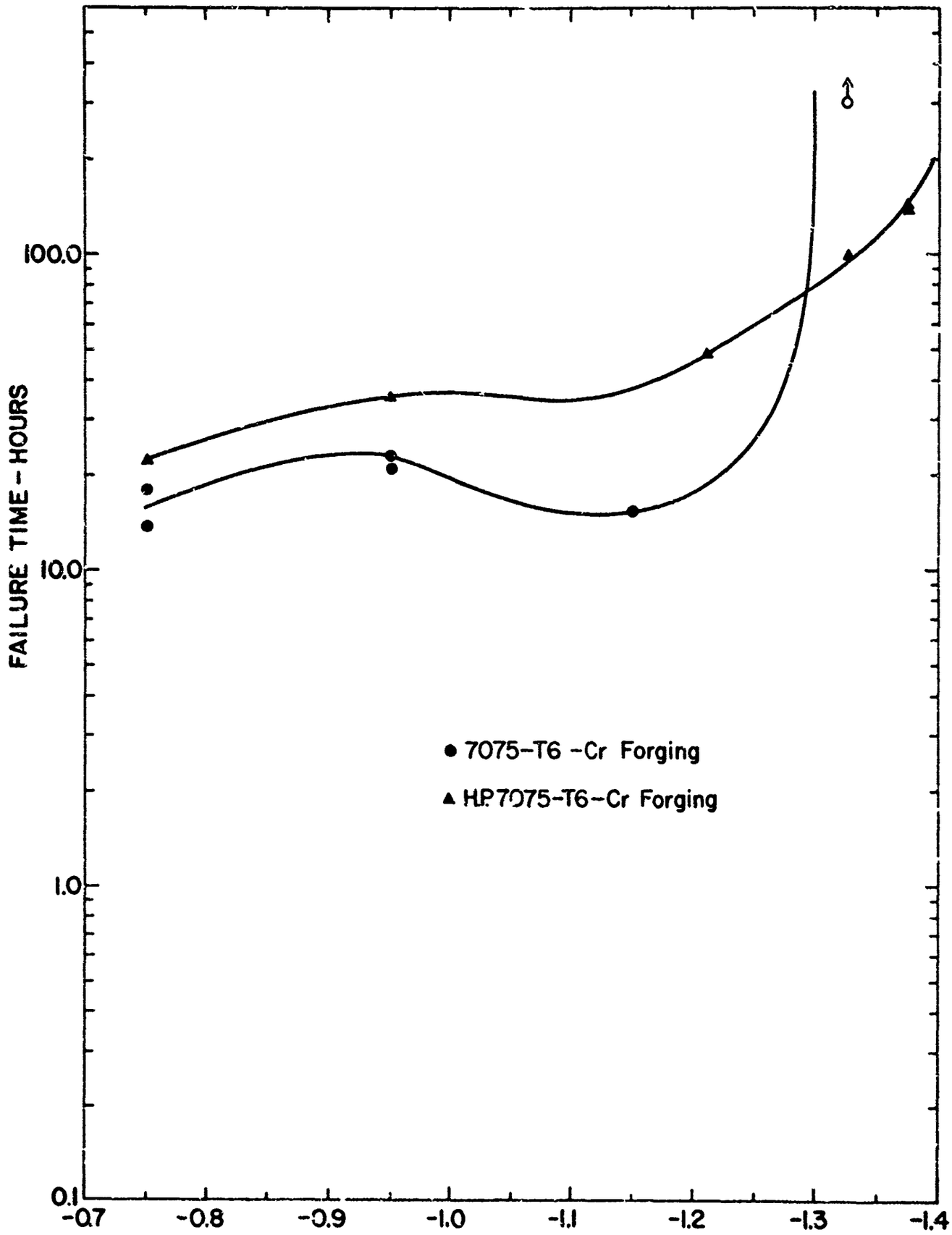
100.0
10.0
1.0
0.1
FAILURE TIME - HOURS
-0.7
-0.8
-0.9
-1.0
-1.1
-1.2
-1.3
-1.4
POTENTIAL - VOLTS VS. SCE
● 7075-T6 -Cr Forging
▲ H.P. 7075-T6-Cr Forging

Figure 6

Figure 7

Resistance-time curve for a tensile specimen of 7075-T6 alloy stressed to 75%Y.S. and exposed at -0.950 volts. The figure illustrates the first stage of the resistance vs. time curve for a specimen failing by stress corrosion: the curve coincides with that for unstressed specimens. At -0.950 volts the second and third stages are both relatively short: they are represented hypothetically by the broken line rising above the experimental curve during the last few minutes of the life.

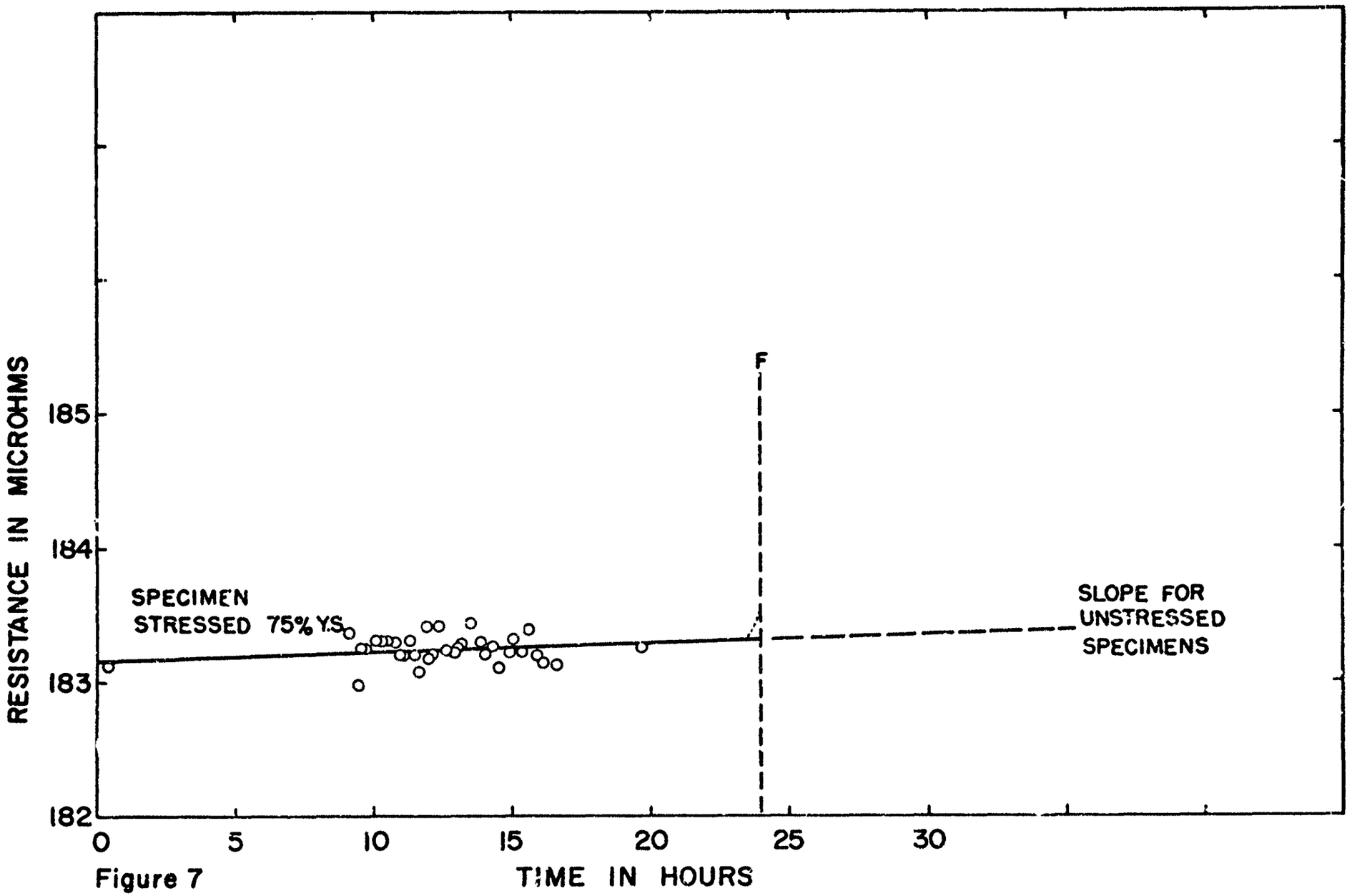
RESISTANCE IN MICROHMS
185
184
183
182
0
5
10
15
20
25
30
TIME IN HOURS
F
SPECIMEN
STRESSED 75% Y.S.
SLOPE FOR
UNSTRESSED
SPECIMENS

Figure 7

Figure 8

Resistance-time curves for tensile specimens of 7075-T6 alloy, stressed to (a) 75%Y.S., (b) 60%Y.S. and (c) 50%Y.S., respectively, and exposed at -1.150 volts. Figure 8 (c) illustrates all three stages of the resistance-time curve.

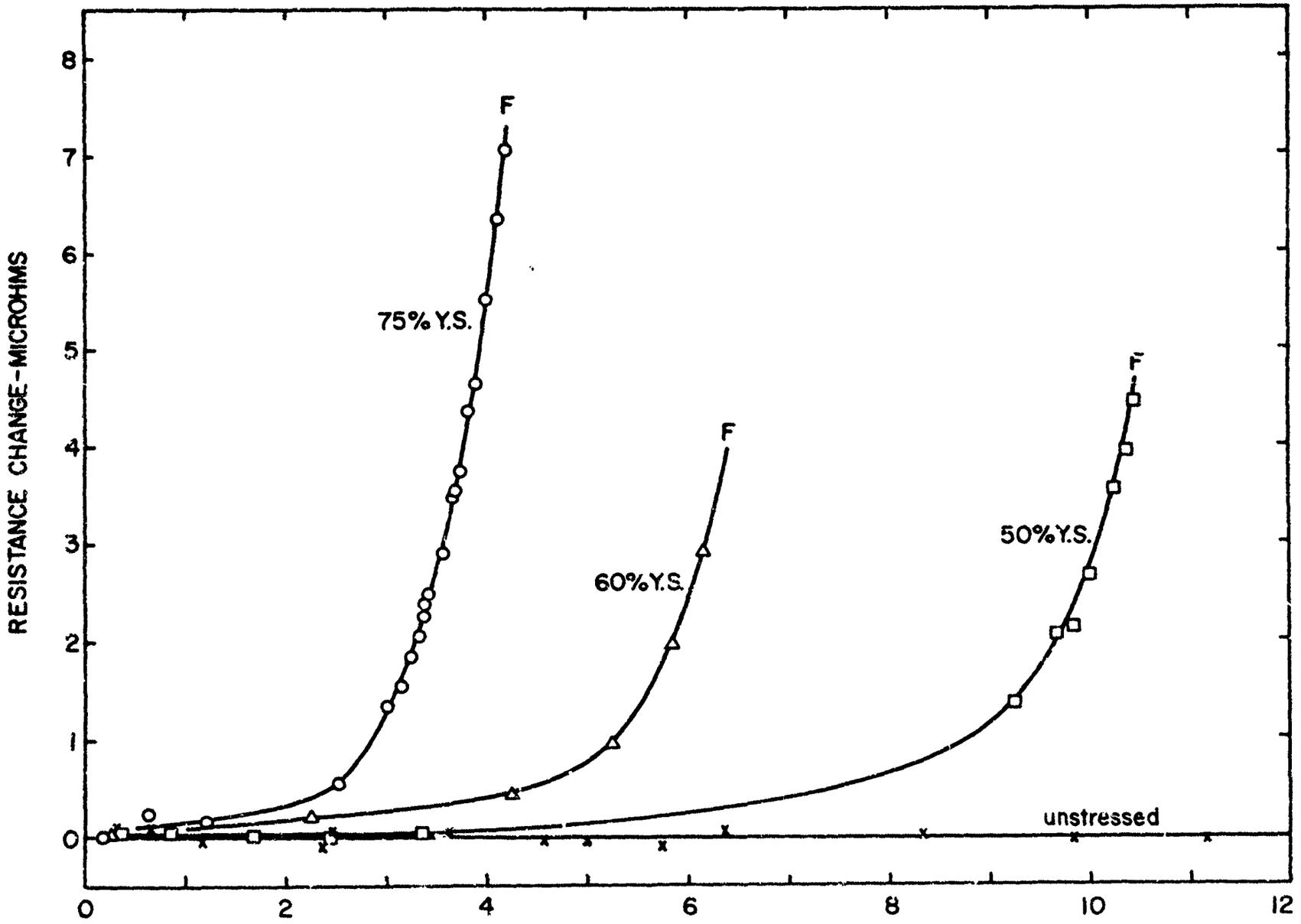
RESISTANCE CHANGE-MICROHMS
LIFETIME— HOURS
75% Y.S.
60% Y.S.
50% Y.S.
unstressed
F
F
F
0
1
2
3
4
5
6
7
8
0
2
4
6
8
10
12

Figure 8

Figure 9

Resistance-time curve for a tensile specimen of 7075-T6 alloy stressed to 75%Y.S. and exposed at -1.150 volts. The figure illustrates the second and third stages of the resistance vs time curve for a specimen failing by stress corrosion: the curve has a finite linear slope for the first three hours (compared with a virtually zero slope for unstressed specimens - not shown) and then resistance increases at an exponential rate until the specimen fails. The first stage of the curve apparently occupies only a few minutes at a potential of -1.150 volts and is not indicated.

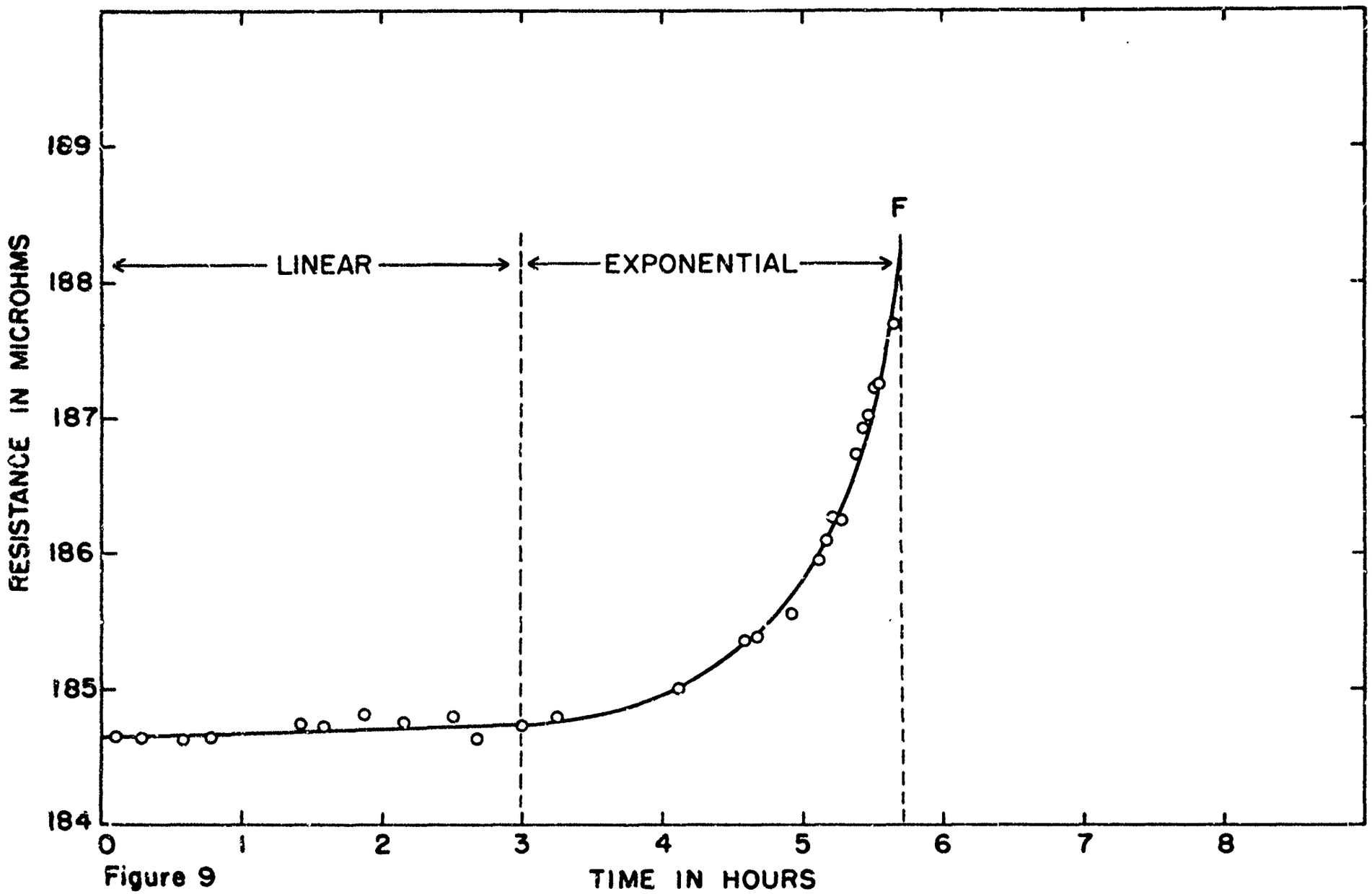
189
188
187
186
185
184
RESISTANCE IN MICROHMS
LINEAR
EXPONENTIAL
F
0
1
2
3
4
5
6
7
8
TIME IN HOURS

Figure 9

Figure 10

Partial resistance-time curves for tensile specimens of 7075-T6 alloy, stressed to (a) 75%Y.S., (b) 60%Y.S. and (c) 50%Y.S., respectively, and exposed at -1.150 volts. The data are the same as those in Figure 8, but plotted on semilogarithmic axes; they demonstrate that the slope of the third stage is independent of initial stress.

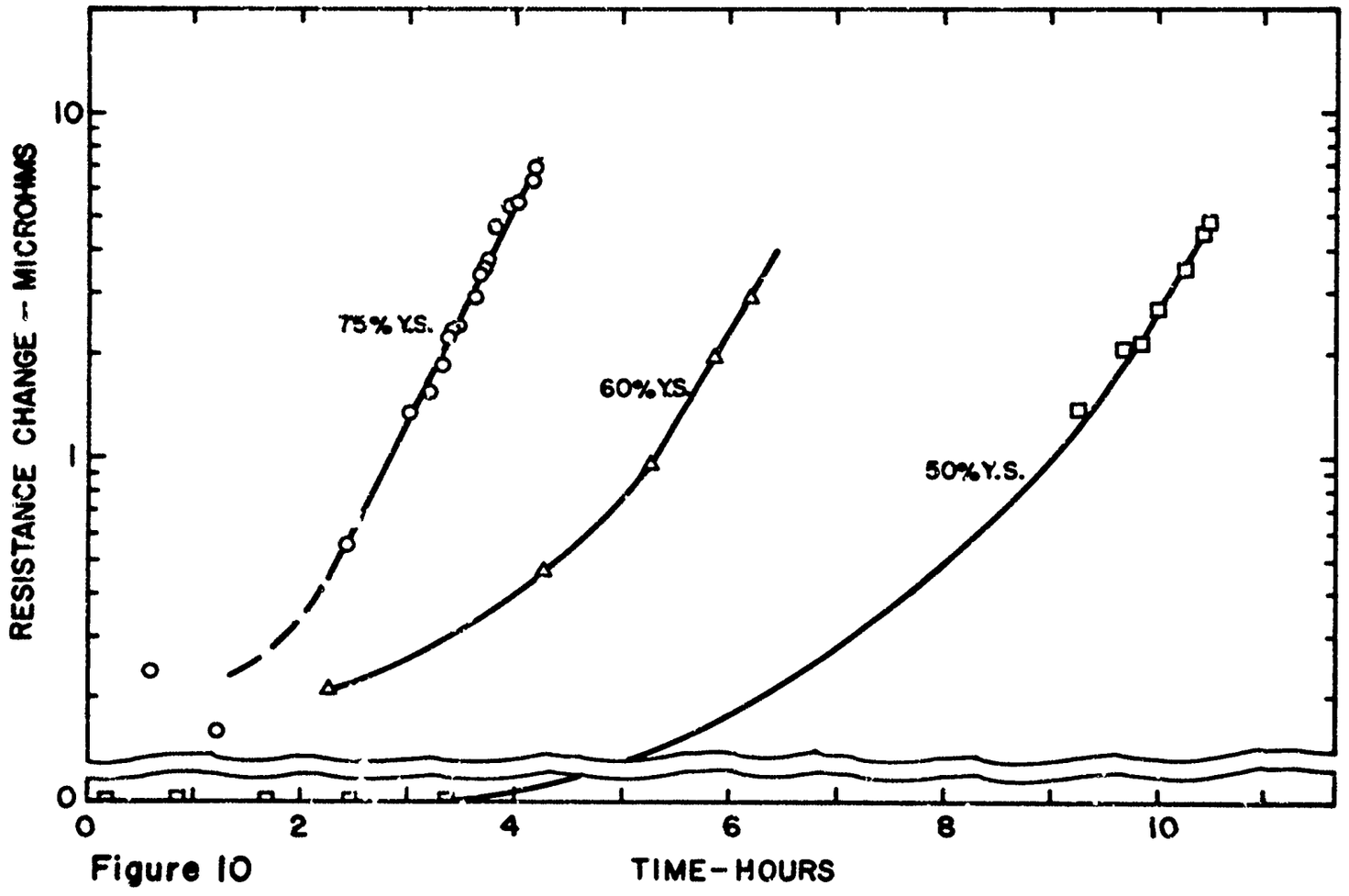
RESISTANCE CHANGE – MICROHMS
10
1
0
75% Y.S.
60% Y.S.
50% Y.S.
0
2
4
6
8
10
TIME – HOURS

Figure 10

Figure 11

Partial resistance-time curves for tensile specimens of high purity 7075-T6 stressed to 75%Y.S. and exposed at various potentials. As the potential becomes more negative, the slope of the curves decreases.

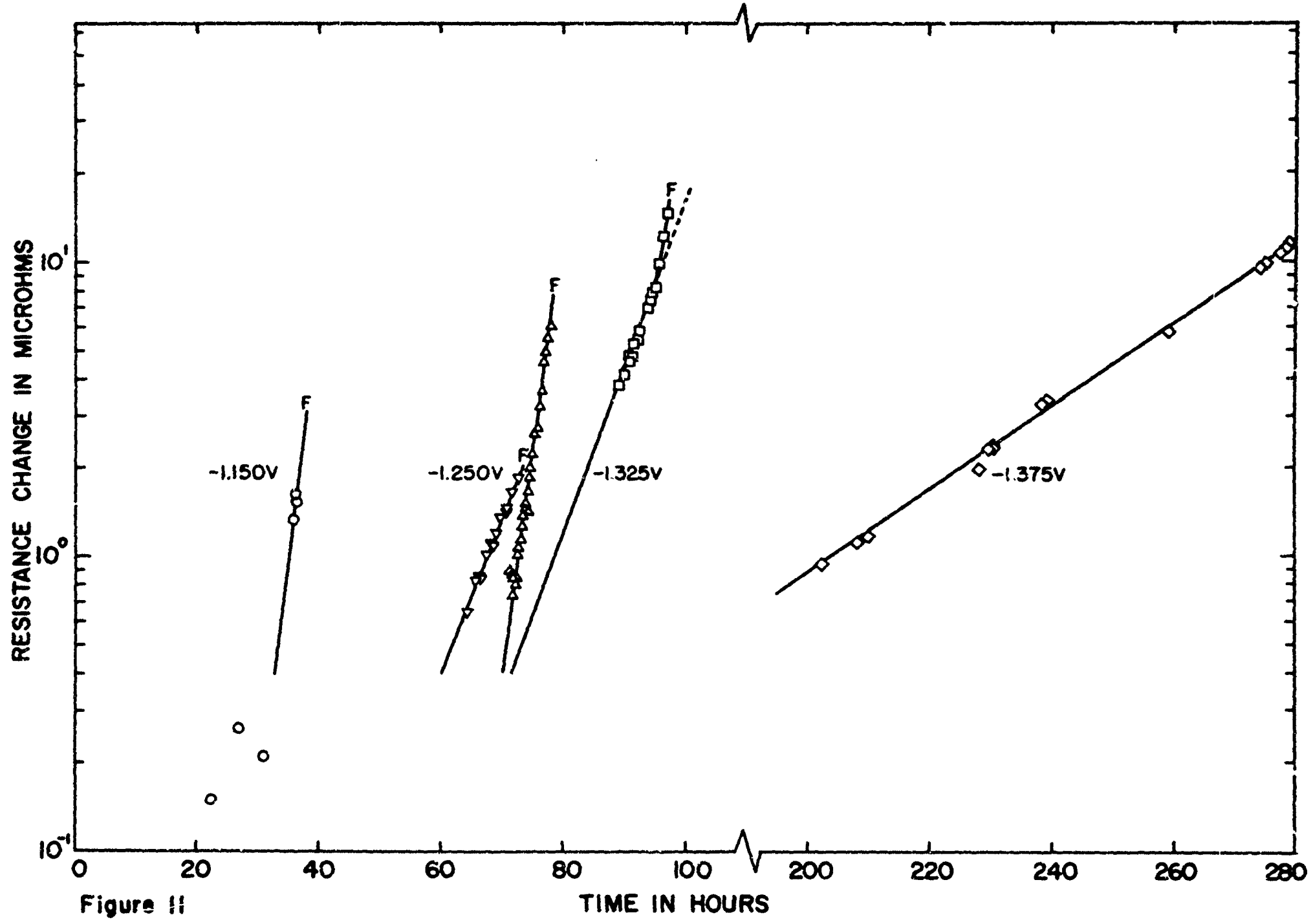
RESISTANCE CHANGE IN MICROHMS
$10^1$
$10^0$
$10^{-1}$
F
-1.150V
-1.250V
-1.325V
-1.375V
0
20
40
60
80
100
200
220
240
260
280
TIME IN HOURS

Figure 11

Figure 12

Light micrographs of sections through three tensile specimens of nominal 7075-T6 alloy forging that failed by stress-corrosion cracking at -0.750 V (free corrosion), -0.950 V, and -1.150 V, respectively. A few small cracks, originating from pits, were observed in specimen N15. Only one crack was observed in specimen N5 and it is the one indicated. At least six cracks were observed in specimen N6 but only one of them is illustrated. Cracks are indicated in each case by arrows (Keller's etch).

NOMINAL 7075-T6 ALLOY

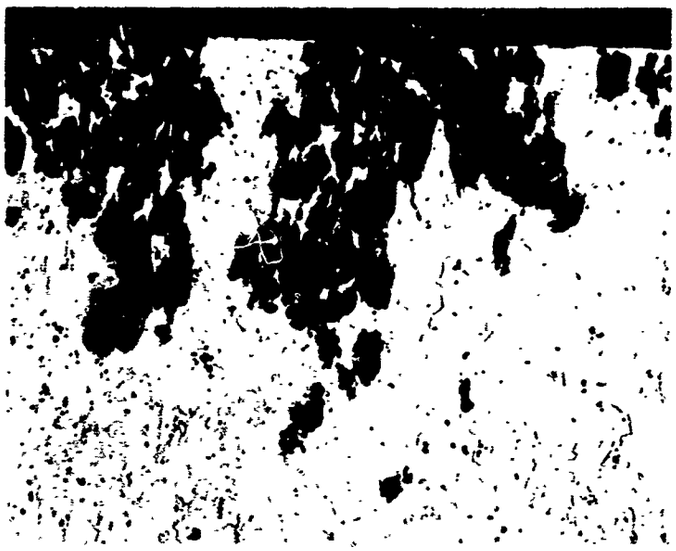

S-321852-N15 -0.750 v/24.0 hrs.

Neg. 147033

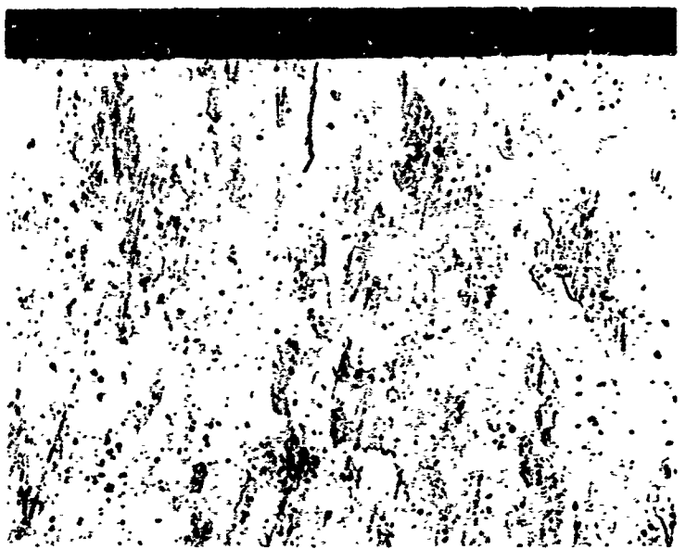

S-321852-N5 -0.950 v/83.8 hrs.

Neg. 147034

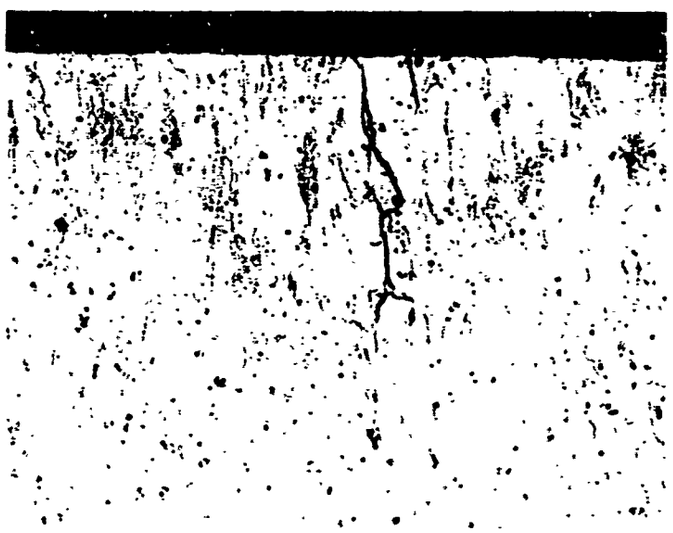

S-321852-N6 -1.150 v/22.7 hrs.

Neg. 147035

PEC 107.1

0.01"

Figure 12

Figure 13

Light micrographs of sections through four tensile specimens of recrystallized 7075-T6 alloy forging that failed by stress-corrosion cracking at -0.750 V (free corrosion), -0.950 V, -1.150 V and -1.325 V, respectively. The results are very similar to those in Figure 12: a few small cracks originated from pits in specimen N6; no cracks were apparent in specimen N4 and several cracks developed in specimen N5. The main difference is that no failure occurred at -1.325 volts with the "nominal 7075-T6" alloy in Figure 12; many short fine cracks like the one indicated were observed in specimen N7 (Keller's etch).

Figure 14

Light micrographs of sections through four tensile specimens of high purity 7075-T6 alloy forging that failed by stress-corrosion cracking at -0.750 V (free corrosion) -0.950 V, -1.150 V and -1.375 V, respectively. As before, cracks in the free corrosion specimen - N6 - originated from pits, and the -0.950 V specimen had the fewest cracks (Keller's etch).

HIGH PURITY 7075-T6 ALLOY

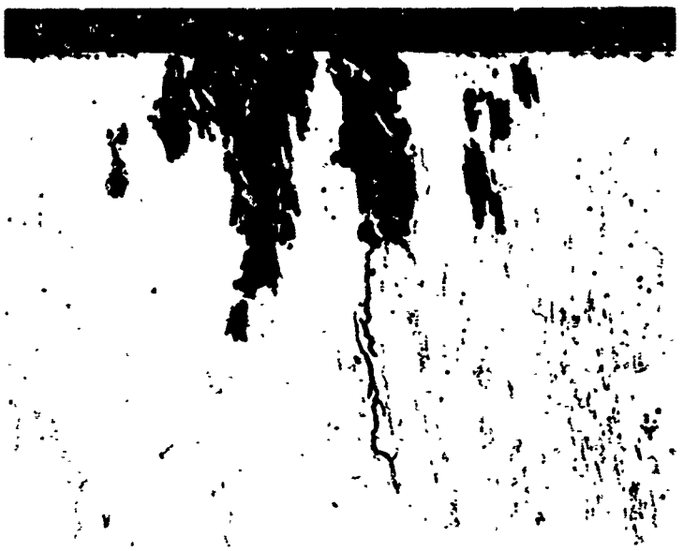

S-321854-N6 -0.750v/26.8 hrs.

Neg. 147040

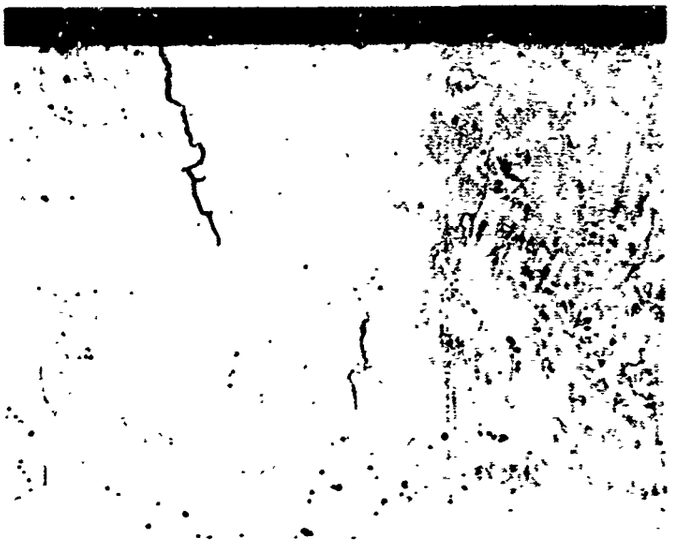

S-321854-N14 -0.950v/82.2 hrs.

Neg. 147041

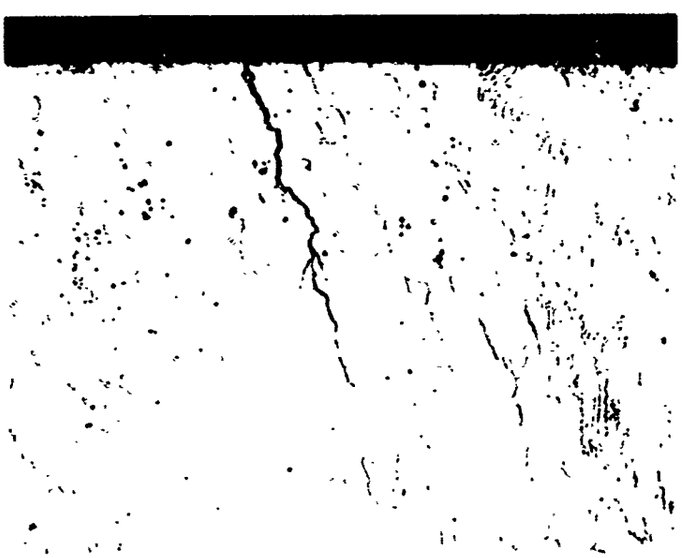

S-321854-N7 -1.150v/48.0 hrs.

Neg. 147042

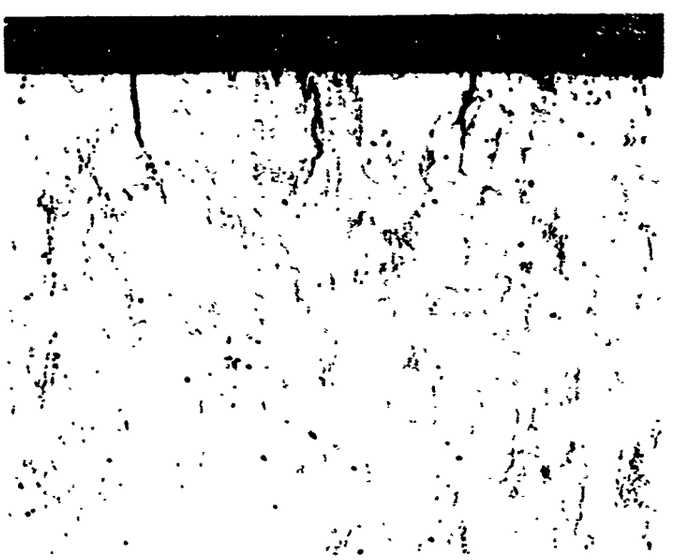

S-321854-N5 -1.375v/144.0 hrs.

Neg. 147044

0.01"

PEC308.1

Figure 14

Figure 15

Light micrographs of sections through three tensile specimens of nominal 7075-T6 - Cr alloy forging that failed by stress-corrosion cracking at -0.750 V (free corrosion), -0.950 V and -1.150 V, respectively. The pitting in specimen N34 was shallower and generally more rounded than that in the previous figures, and fewer cracks originated from the pits. The -0.950 V specimen again showed only one or two cracks, compared with at least five in the -1.150 V specimen (Keller's etch).

NOMINAL 7075-T6-Cr ALLOY

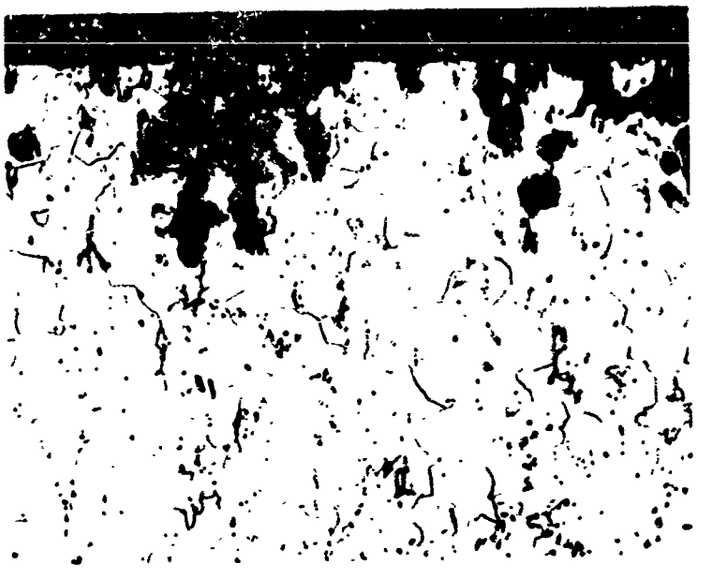

S-321615-N34 -0.750v/13.7 hrs.

Neg. 147049

S-321615-N16 -0.950v/21.8 hrs.

Neg. 147050

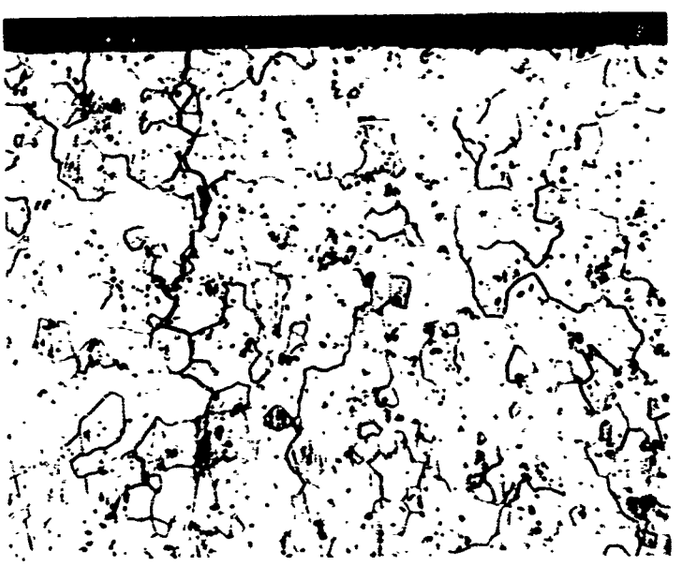

S-321615-N17 -1.150v/15.5 hrs.

Neg. 147051

0.01"

PEC311J

Figure 15

Figure 16

Light micrographs of sections through four tensile specimens of high purity 7075-T6 - Cr alloy forgings that failed by stress-corrosion cracking at -0.750 V (free corrosion), -0.950 V, -1.325 V and -1.375 V. As in Figure 15, the pits formed at -0.075 V were shallow and rounded. In specimen N8, no visible cracks originated from the pits. Specimen N28 also contained no cracks, but specimens N6 and N33 contained many cracks (Keller's etch).

HIGH PURITY 7075-T6-Cr ALLOY

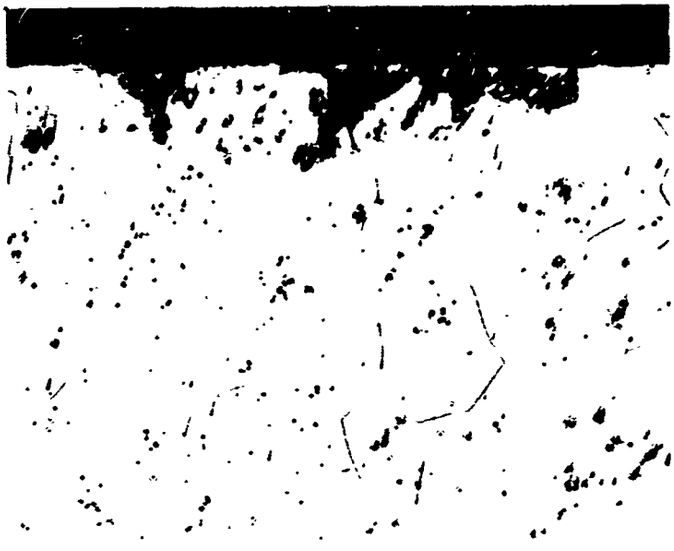

S-321780-N8 -0.750v/22.5 hrs.

Neg. 147045

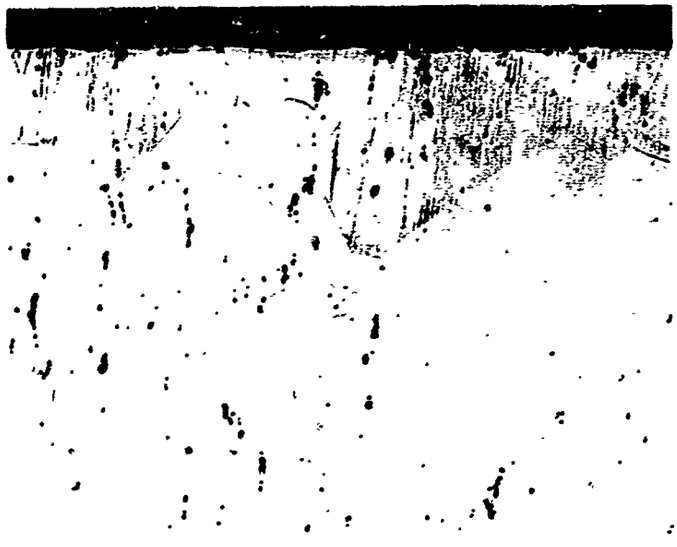

S-321780-N28 -0.950v/35.5 hrs.

Neg. 147046

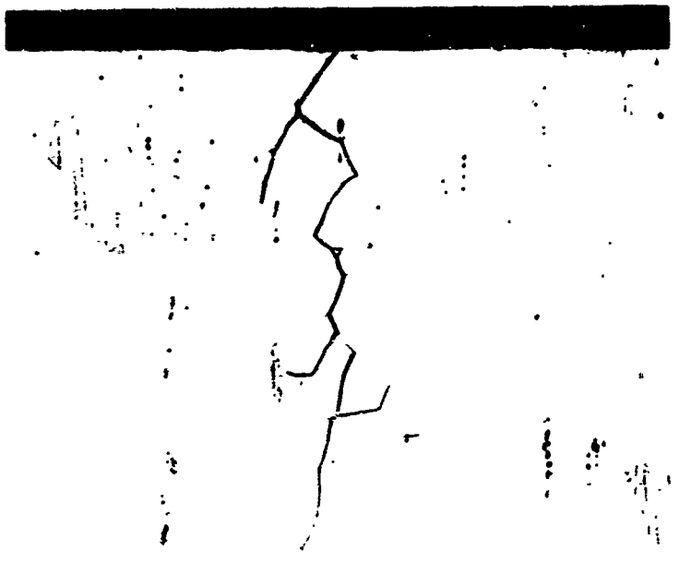

S-321780-N6 -1.325v/98.2 hrs.

Neg. 147047

S-321780-N33 -1.375v/138.8 hrs.

Neg. 147048

PEC2063

0.01"

Figure 16

Figure 17

Oxide replica of a prepolished specimen of 7075-T6 alloy plate exposed unstressed at free corrosion (about -0.750 volts) for 2 hours. The large dark area was a corrosion pit. Only mild attack was apparent over the remainder of the surface (the 'matrix'). In preparing the micrographs in Figures 17 - 38, specimens were metallographically polished and then corroded. After corrosion, specimens were cleaned in nitric acid or a hot chromic-phosphoric acid stripping solution, to remove corrosion product. The oxide replicas were formed in a 3% tartaric acid solution adjusted to pH 5 with ammonium hydroxide.

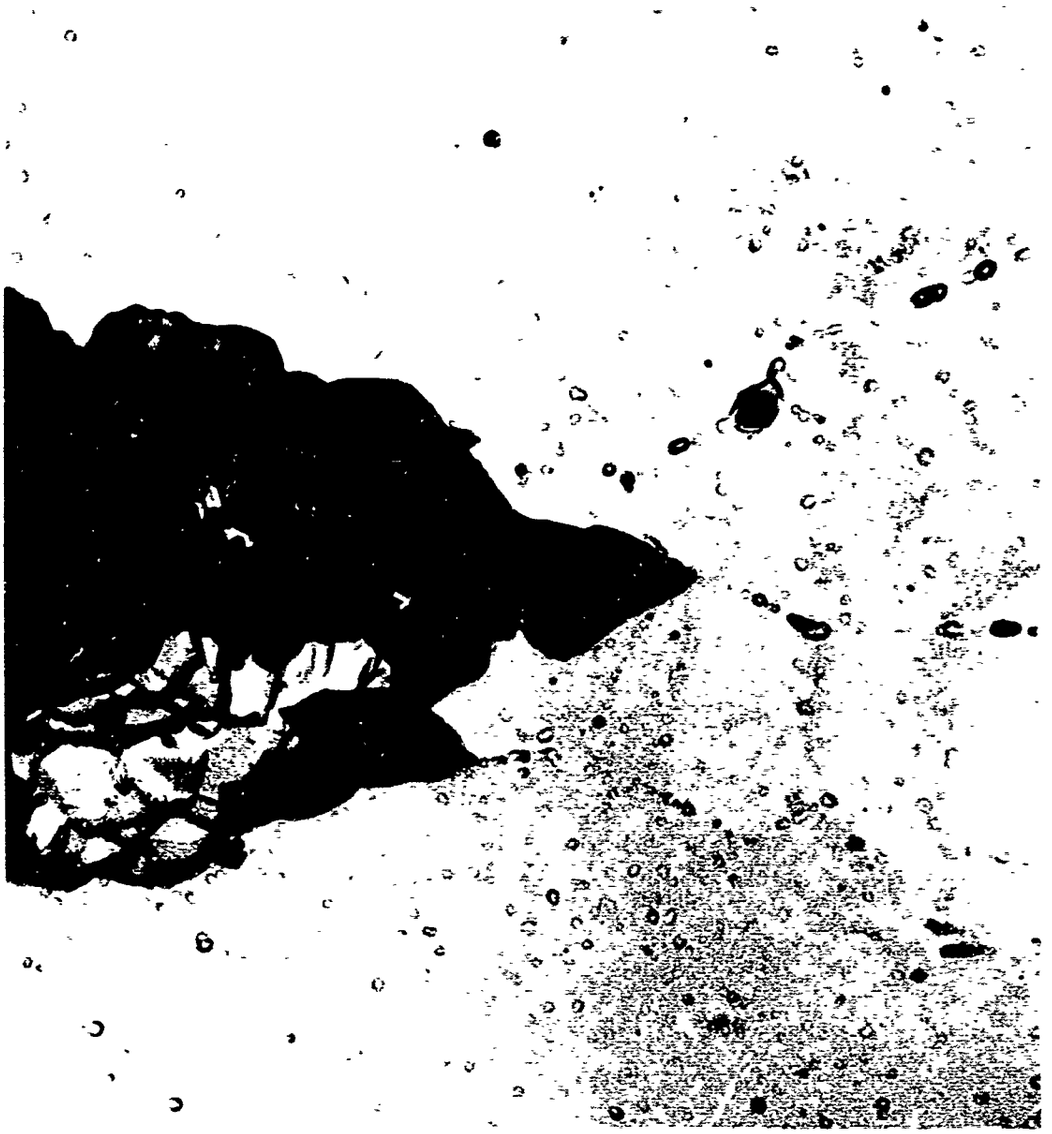

S-320831-E7 Neg. 153/10/6 10,000X

7075-T6 Unstressed -0.750 V/2 Hrs.

Figure 17

Figure 18

Oxide replica of a prepolished specimen of 7075-T6 alloy plate exposed unstressed at -0.950 volts for 22.25 hours. The large corrosion pit was similar to that in Figure 17, but there was considerably more severe attack of the matrix. (Note, however, the difference in the times of exposure.)

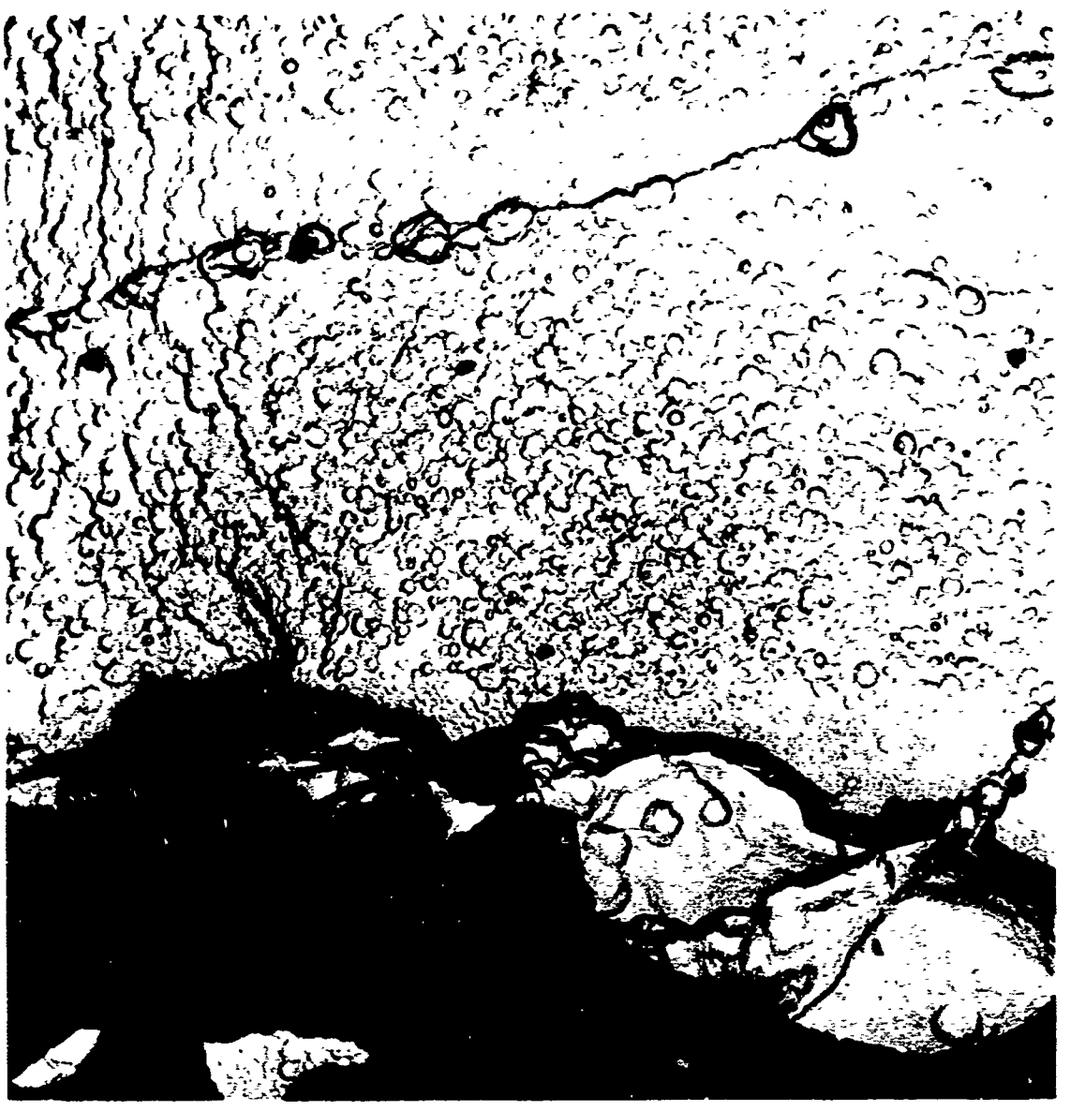

S-320831-E10A Neg. 150/6/3 10,000X

7075-T6 Unstressed -0.950 V/22.25 Hrs.

Figure 18

Figure 19

Oxide replica of a prepolished specimen of 7075-T6 alloy plate exposed unstressed at -1.150 volts for 23 hours. Large corrosion pits like the one in the next figure were found, but were considerably less common than in the specimen exposed at -0.950 volts. The attack on the matrix - shown here - was slightly less than in Figure 18.

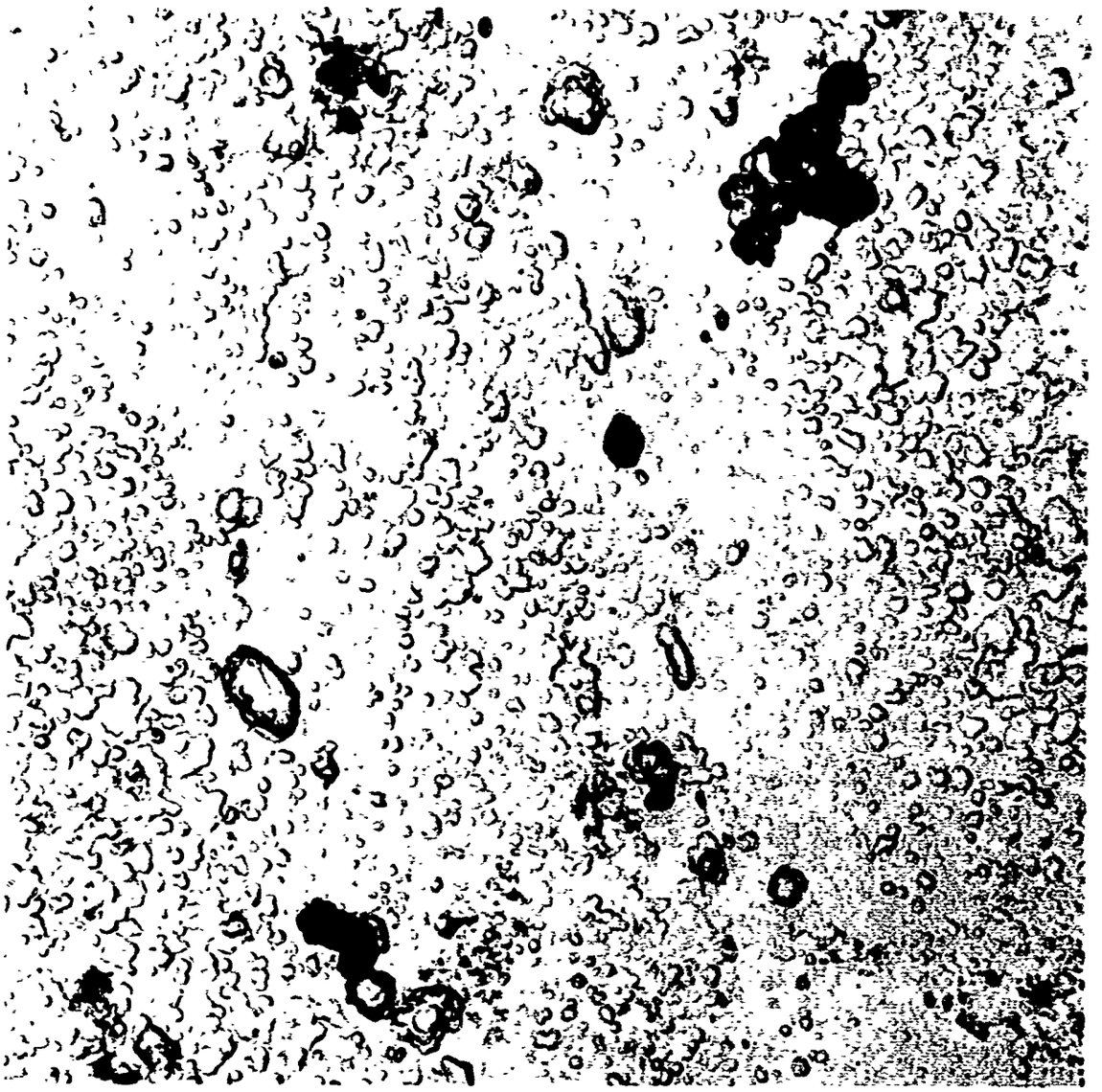

| | | |
|---|---|---|
| S-320831-E3 | Neg. 145/3/2 | 10,000X |
| 7075-T6 | Unstressed | -1.150 V/23 Hrs. |

**Figure 19**

Figure 20

Oxide replica of a prepolished specimen of 7075-T6 alloy plate exposed unstressed at -1.250 volts for 22 hours. Occasional large corrosion pits like that at "A" were found. The attack on the matrix was very mild.

S-320831-E5 Neg. 145/4/2 10,000X

7075-T6 Unstressed -1.250 V/22 Hrs.

Figure 20

Figure 21

Oxide replica of a prepolished specimen of 7075-T6 alloy plate exposed unstressed at -1.350 volts for 24 hours. Only very mild attack was found - either associated with the particles (the rounded grey areas) or over the matrix. No large pits were found in this replica.

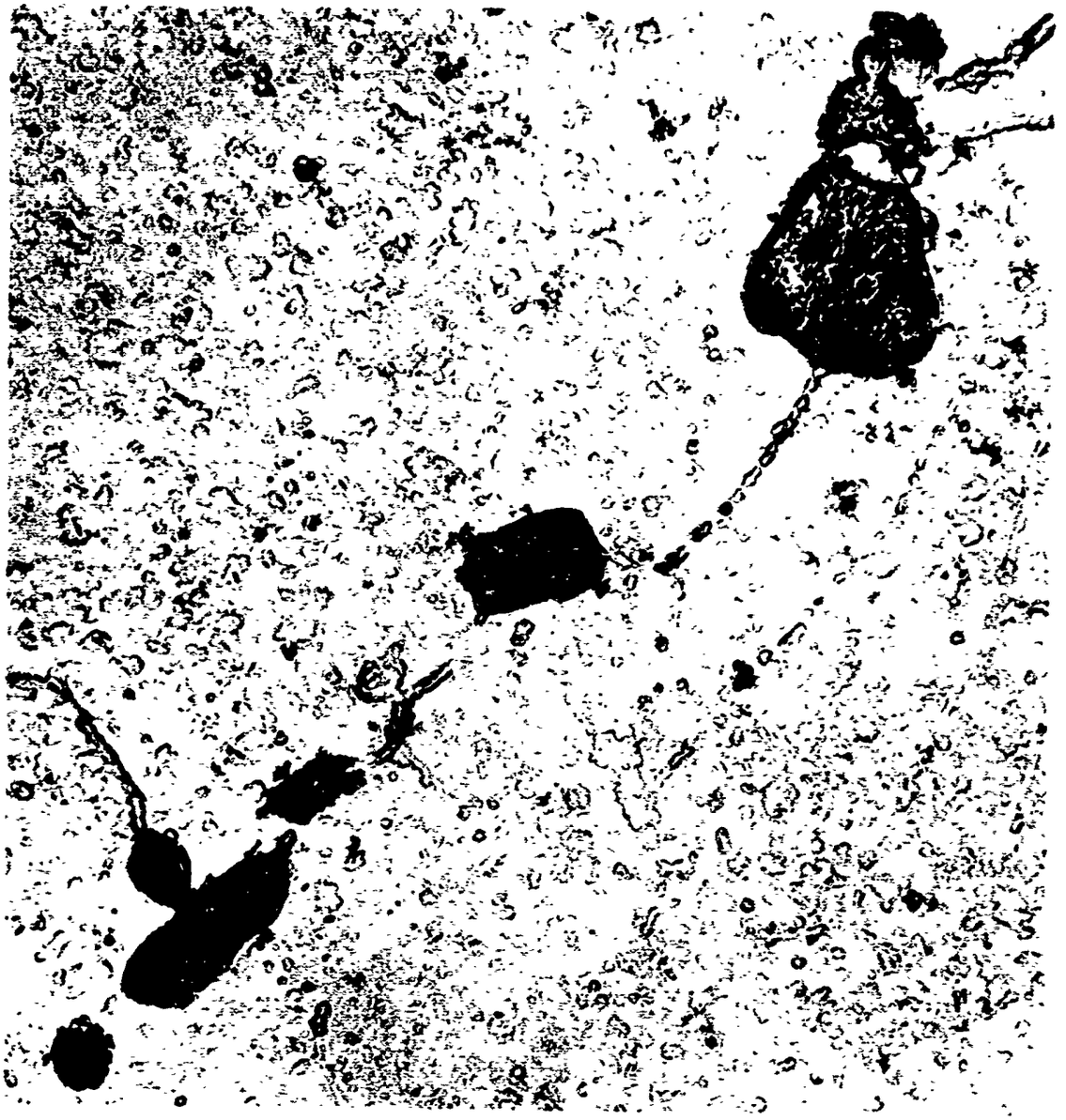

S-320831-E6 Neg. 145/4/6 10,000X

7075-T6 Unstressed -1.350 V/24 Hrs.

Figure 21

Figure 22

Oxide replica of a prepolished specimen of 7075-T6 alloy plate exposed stressed at free corrosion (about -0.750 volts) for 2 hours. The large corrosion pit was similar to the one in the unstressed specimen shown in Figure 17. No sign of cracking along grain boundaries was apparent.

S-320831-E11A Neg. 151/11/3 10,000X

7075-T6 Stressed 75% Y. S. Free Corrosion/2 Hrs.

**Figure 22**

Figure 23

Oxide replica of a prepolished specimen of 7075-T6 alloy plate exposed stressed at -0.950 volts for 18 hours. There was a marked similarity in the attack to that in the equivalent unstressed specimen in Figure 18 (in comparing stressed and unstressed specimens, note the difference in magnification). As in Figure 22, no intergranular cracks had developed during the exposure.

S-320831-E15A Neg. 151/14/4 5,000X

7075-T6 Stressed 75%Y.S. -0.950 V/18 Hrs.

Figure 23

Figure 24

Oxide replica of a prepolished specimen of 7075-T6 alloy plate exposed stressed at -1.150 volts for 5.2 hours. The exposure was shorter than that for any other specimen (except those at free corrosion) because cracks developed so rapidly. An intergranular crack originated on the surface at the line "AB" and extended underneath in a direction corresponding to the bottom of the page. The rounded, discrete regions "C" were constituent particles.

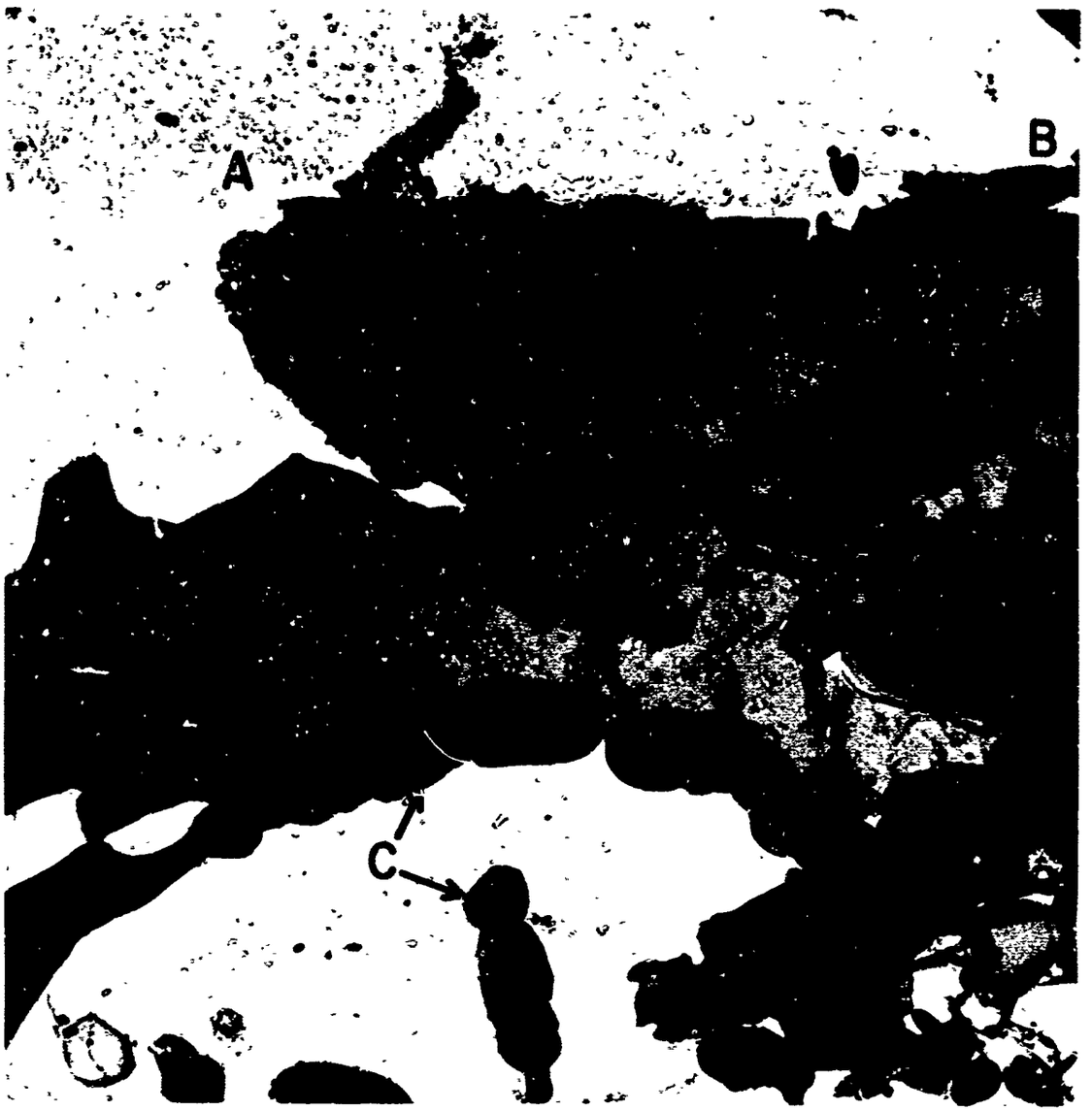


S-320831-E3A Neg. 148/6/3 5,000X

7075-T6 Stressed 75%Y.S. -1.150 V/5.2 Hrs.

Figure 24

Figure 25

Oxide replica of a prepolished specimen of 7075-T6 alloy plate exposed stressed at -1.150 volts for 5.2 hours. The micrograph illustrates another area of the same specimen shown in Figure 24. (But note the difference in magnification.) Attention is directed towards the large pit at "A", to the constituent particles "B" adjacent to the pit and to the intergranular crack at "C".

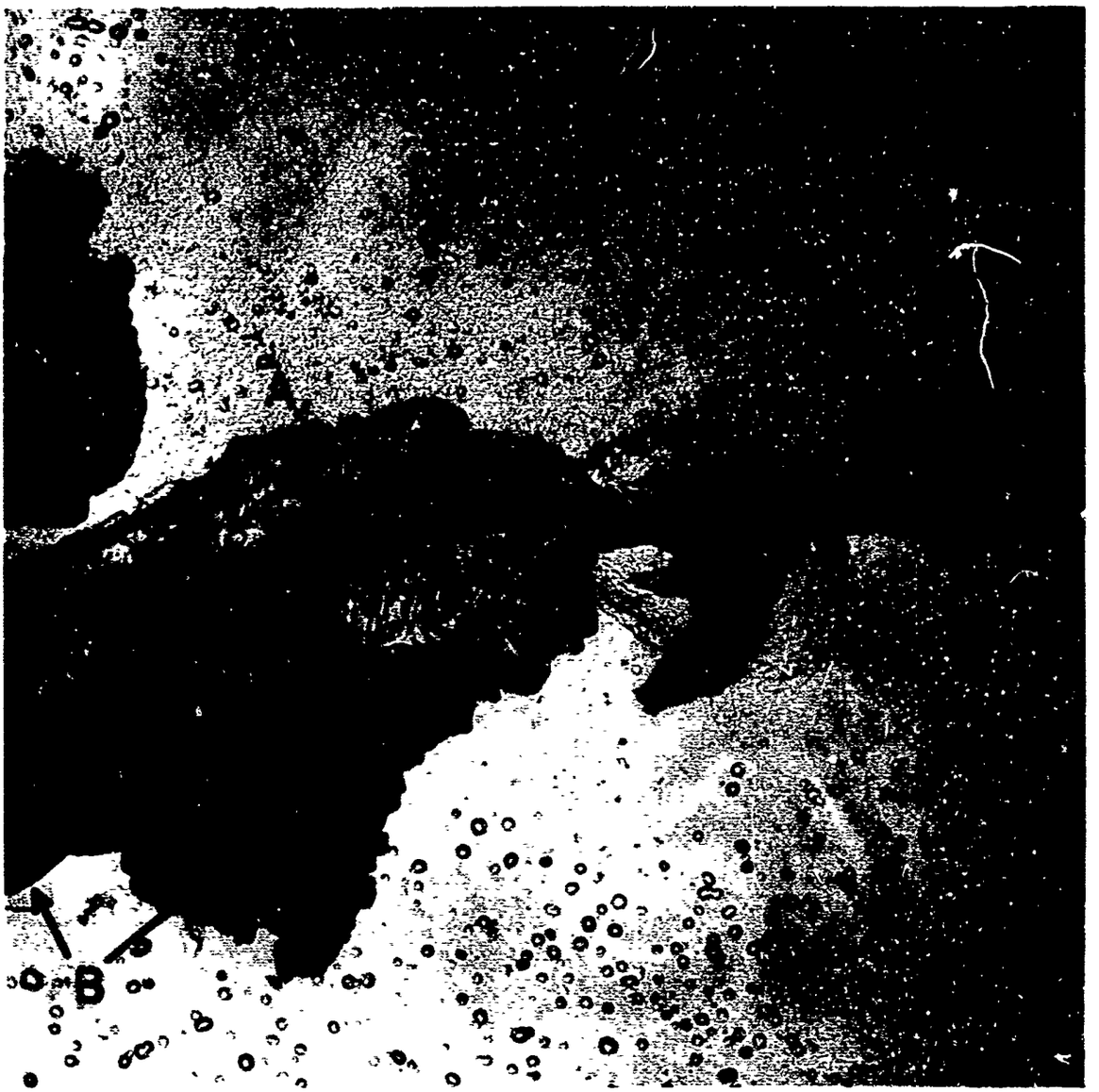


S-320831-E3A Neg. 148/6/1 10,000X

7075-T6 Stressed 75%Y.S. -1.150 V/5.2 Hrs.

Figure 25

Figure 26

Oxide replica of a prepolished specimen of 7075-T6 alloy plate exposed stressed at -1.250 volts for 18 hours. Note that the intergranular crack was associated with a small corrosion pit - "A" - and what may have been constituent particles - "B".

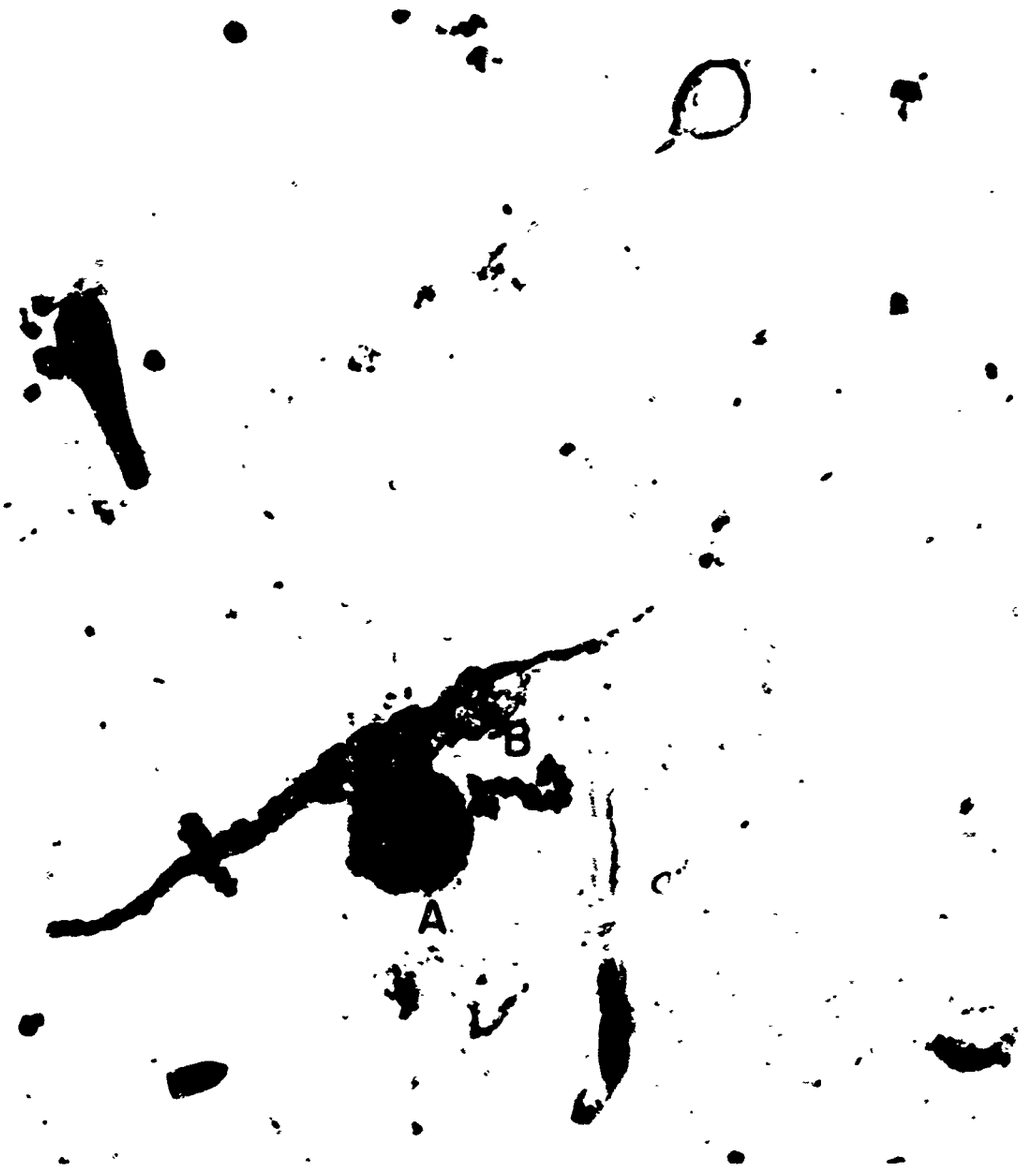


S-320831-E11A Neg. 153/13/1 5,000X

7075-T6 Stressed 75%Y.S. -1.250 V/18 Hrs.

Figure 26

Figure 27

Oxide replica of a prepolished specimen of 7075-T6 alloy plate exposed stressed at -1.350 volts for 18 hours. The specimen developed small intergranular cracks in spite of the fact that the potential was sufficient to provide complete protection for a tensile specimen. As in Figures 24 - 26 a crack developed close to both a corrosion pit and a constituent particle. (The white areas in the micrograph resulted from flaws in the replica. Crack-shaped flaws are also apparent in some of the other micrographs.)

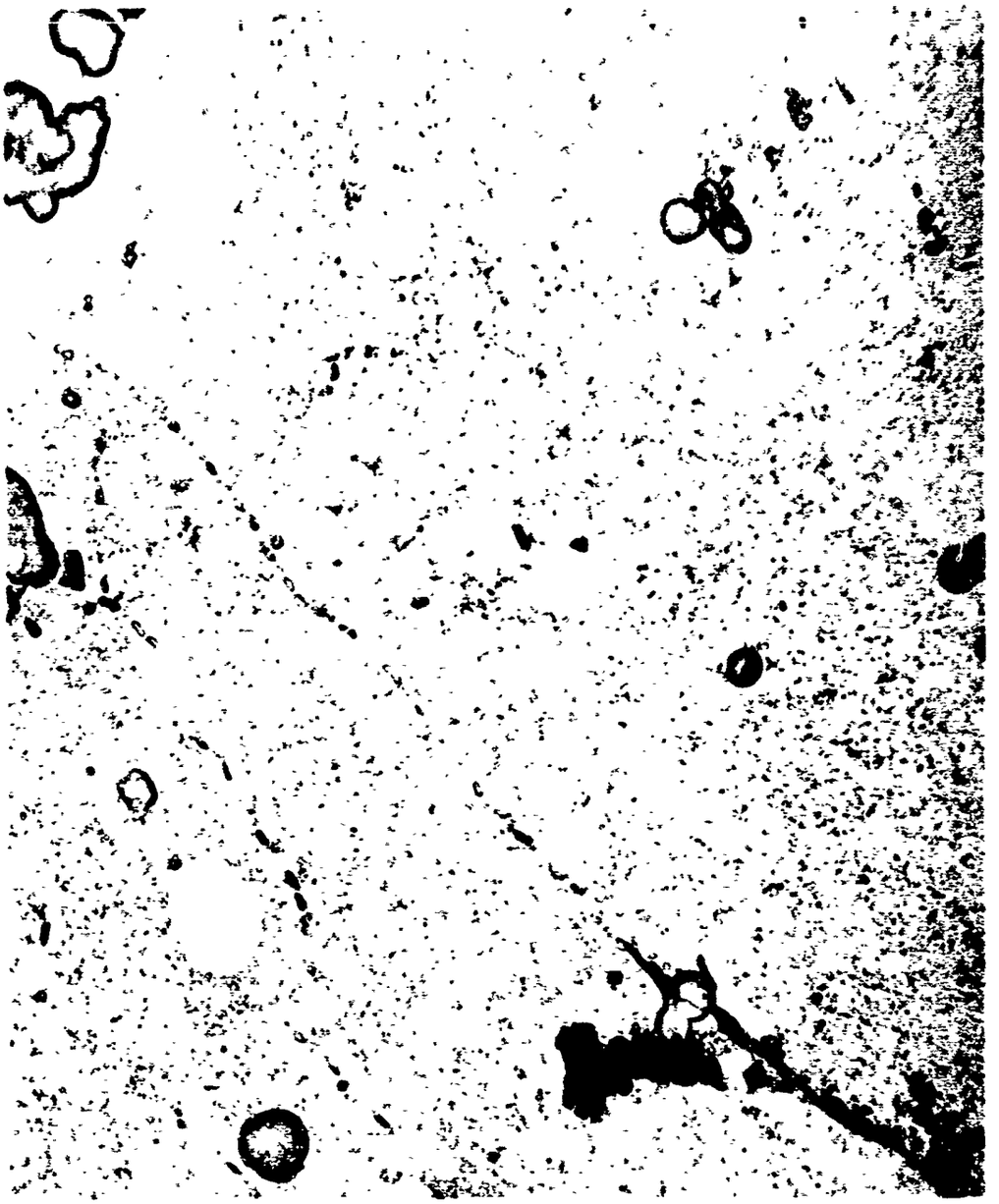

S-320831-E12A Neg. 151/11/7 5,000X

7075-T6 Stressed 75%Y.S. -1.350 V/18 Hrs.

Figure 27

Figure 28

Oxide replica of a prepolished specimen of 7075-T73 alloy plate exposed unstressed at free corrosion (about -0.750 volts) for 2 hours. In contrast to the comparable specimen of 7075-T6 alloy (Figure 17) the pitting attack was of a well defined crystallographic ("cubic") nature, and the matrix was more severely attacked.

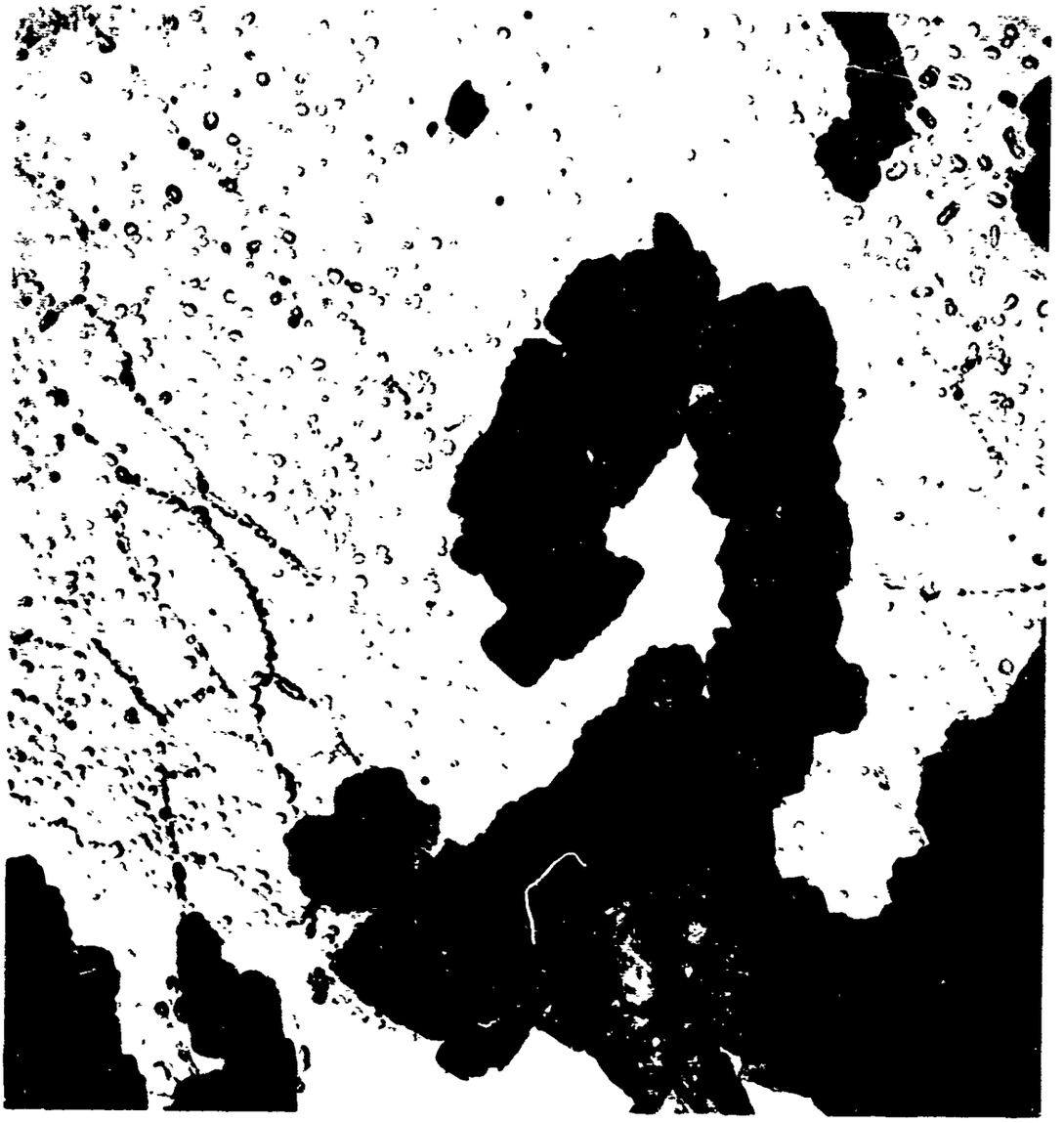

S-320832-E6 Neg. 153/10/8 10,000X

7075-T73 Unstressed -0.750 V/2 Hrs.

**Figure 28**

Figure 29

Oxide replica of a prepolished specimen of 7075-T73 alloy plate exposed unstressed at -1.150 volts for 18 hours. The cubic nature of the pitting is quite apparent.

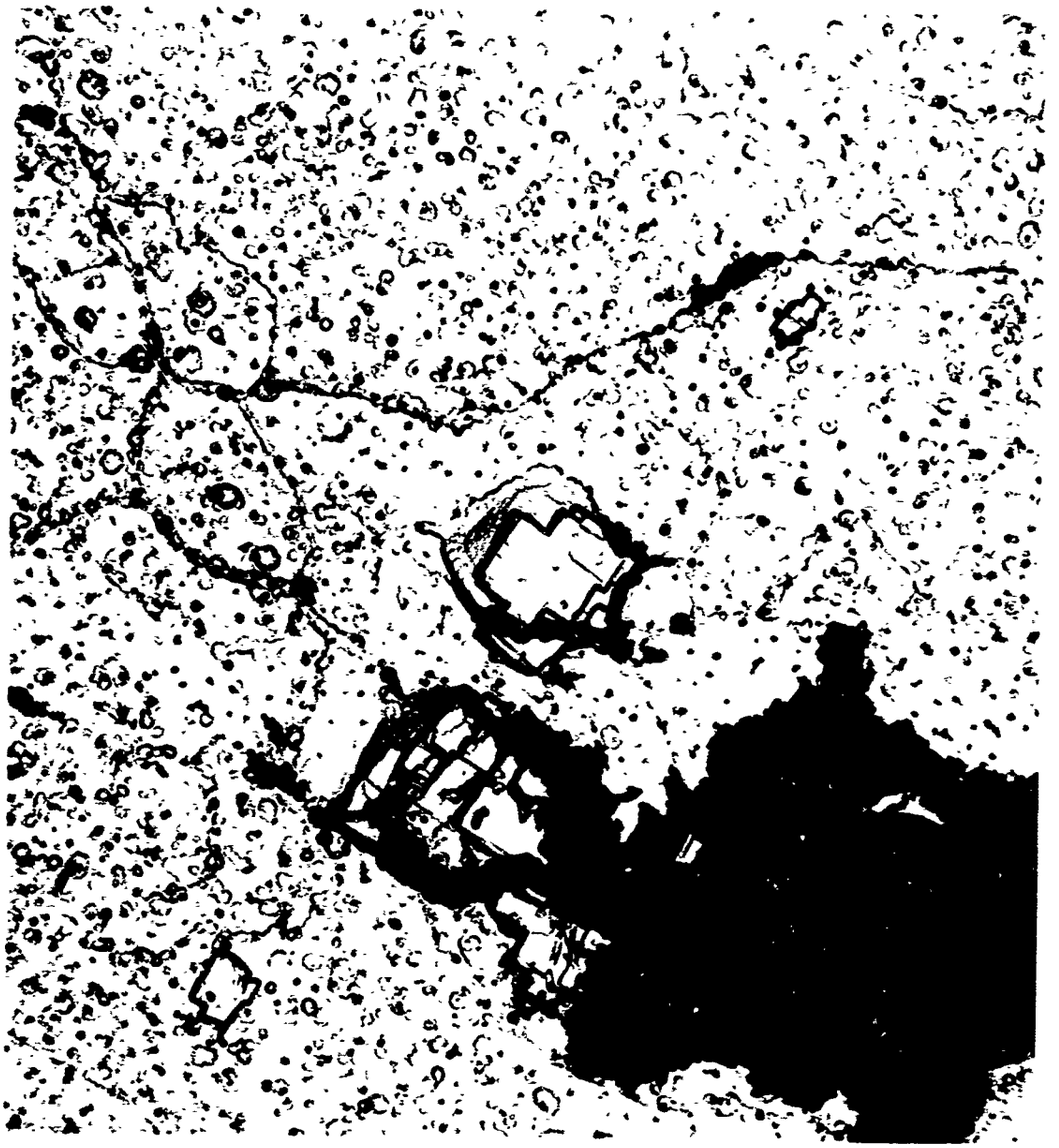

| | | |
|---|---|---|
| S-320832-E3 | Neg. 147/8/8 | 10,000X |
| 7075-T73 | Unstressed | -1.150 V/18 Hrs. |

Figure 29

Figure 30

Oxide replica of a prepolished specimen of 7075-T73 alloy plate exposed unstressed at -1.250 volts for 18 hours. Cubic pits are less in evidence than in Figures 28 and 29 and matrix attack is less severe than in Figure 29.

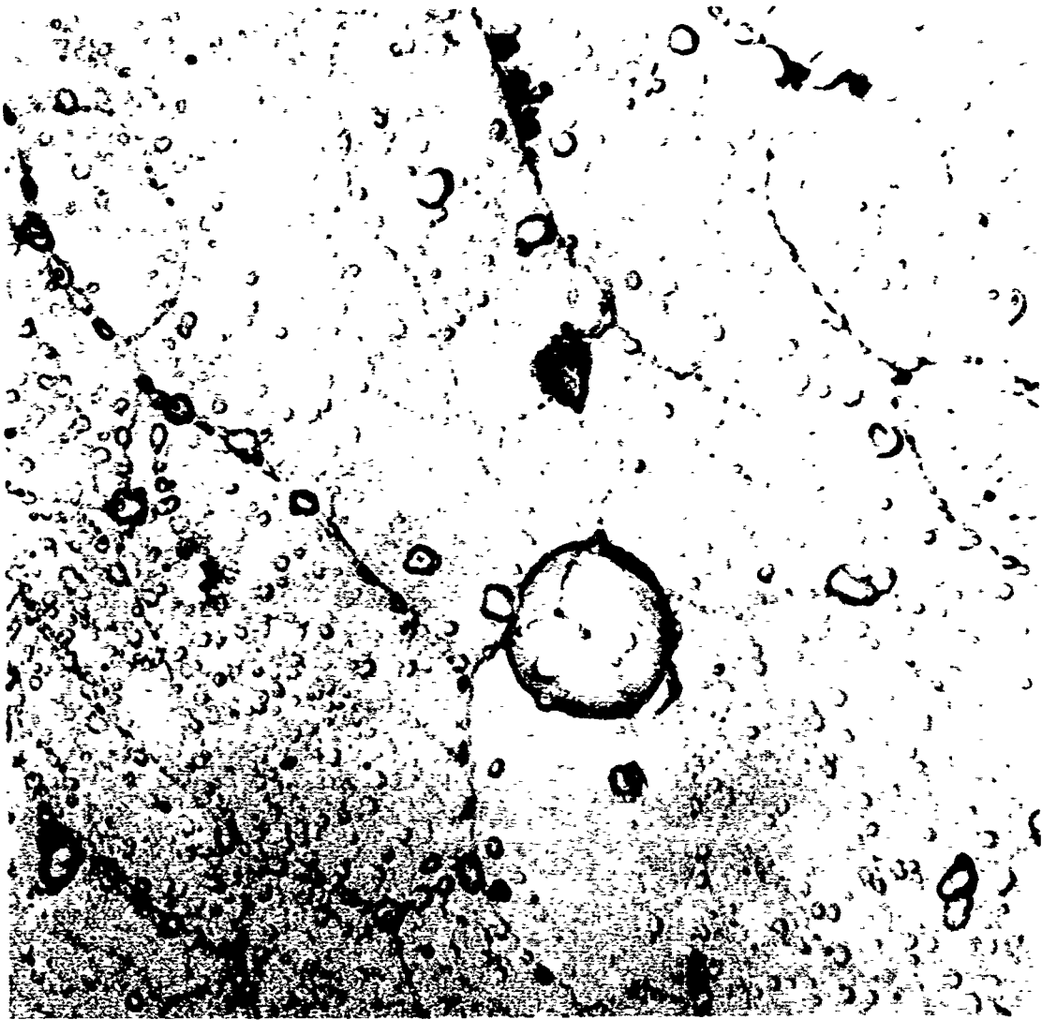

S-320832-E12A | Neg. 152/13/2 | 10,000X

7075-T73 | Unstressed | -1.250 V/18 Hrs.

Figure 30

Figure 31

Oxide replica of a prepolished specimen of 7075-T73 alloy plate exposed unstressed at -1.320 volts for 18 hours. No large pits were found. The specimen exhibited only a slightly roughened surface.

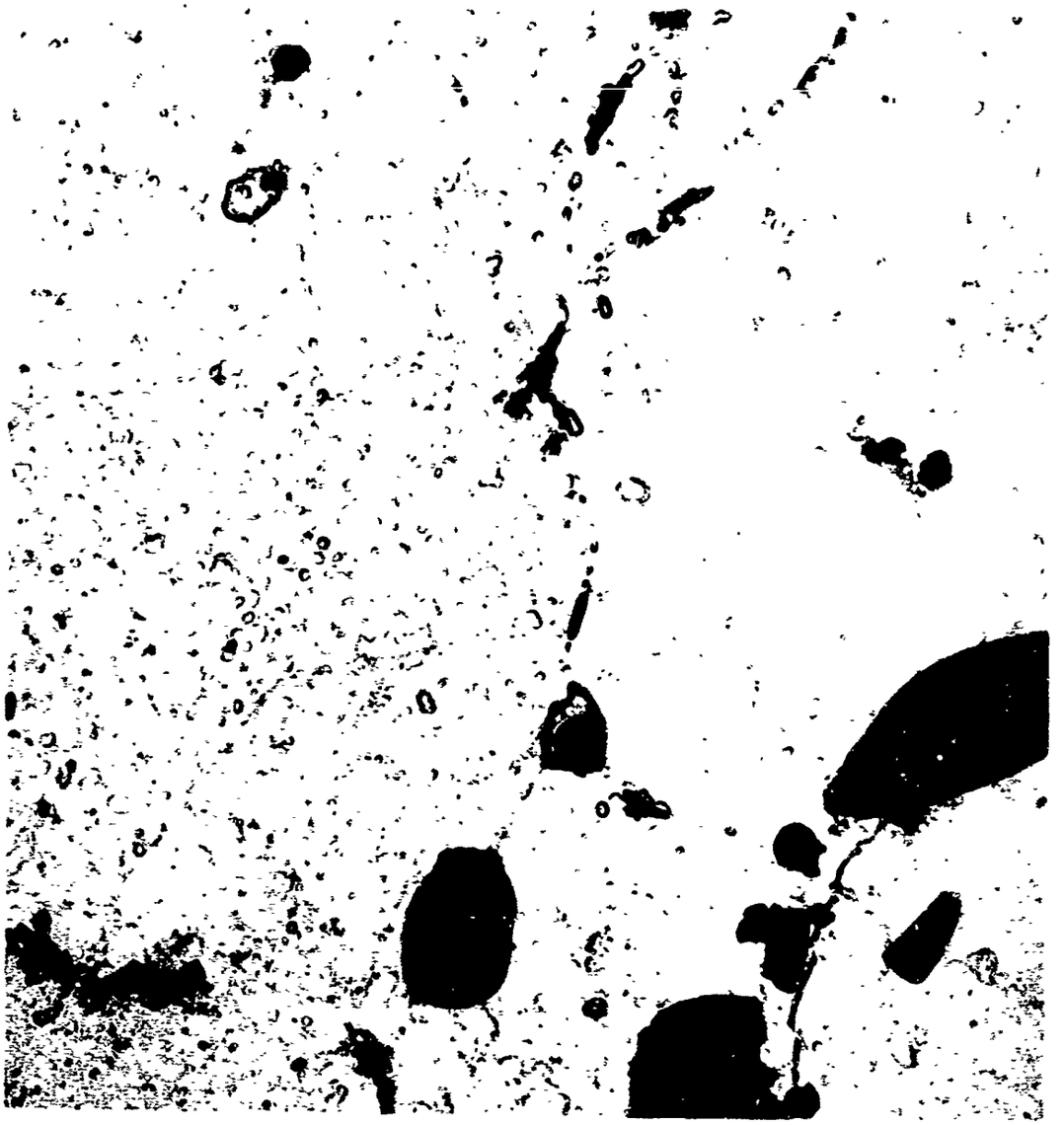

S-320832-E1 Neg. 147/10/3 10,000X

7075-T73 Unstressed -1.320 V/18 Hrs.

Figure 31

Figure 32

Oxide replica of a prepolished specimen of 7075-T73 alloy plate exposed stressed at free corrosion (about -0.750 volts) for 2 hours. Notice the distinct cubic configuration of the pitting, and the similarity in appearance to Figure 28.

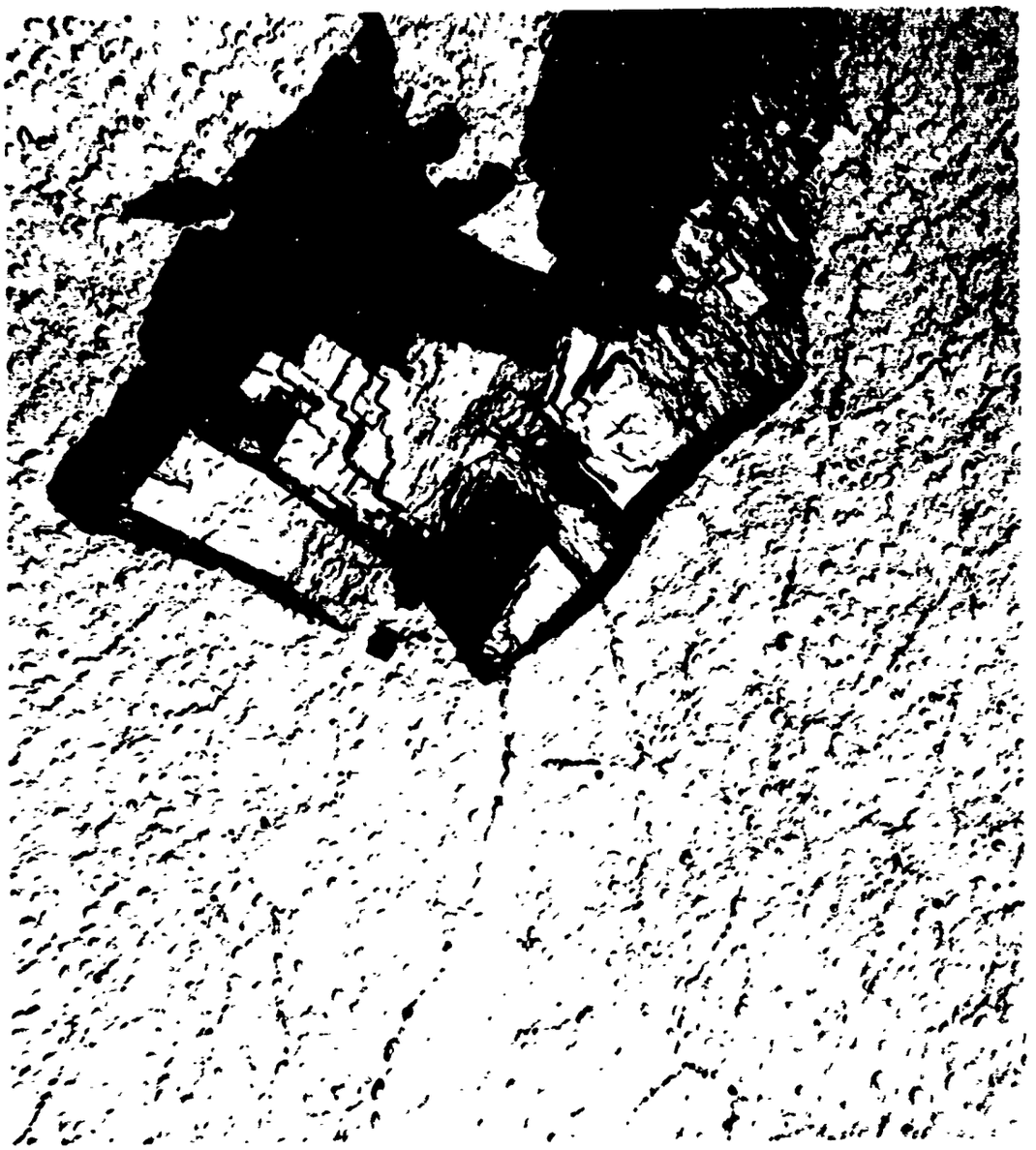

S-320832-E10A Neg. 151/12/3 10,000X

7075-T73 Stressed 75% Y. S. Free Corrosion/2 Hrs.

Figure 32

Figure 33

Oxide replica of a prepolished specimen of 7075-T73 alloy plate exposed stressed at -0.950 volts for 18 hours. There was a strong similarity in matrix attack to other specimens exposed at -0.950 volts.

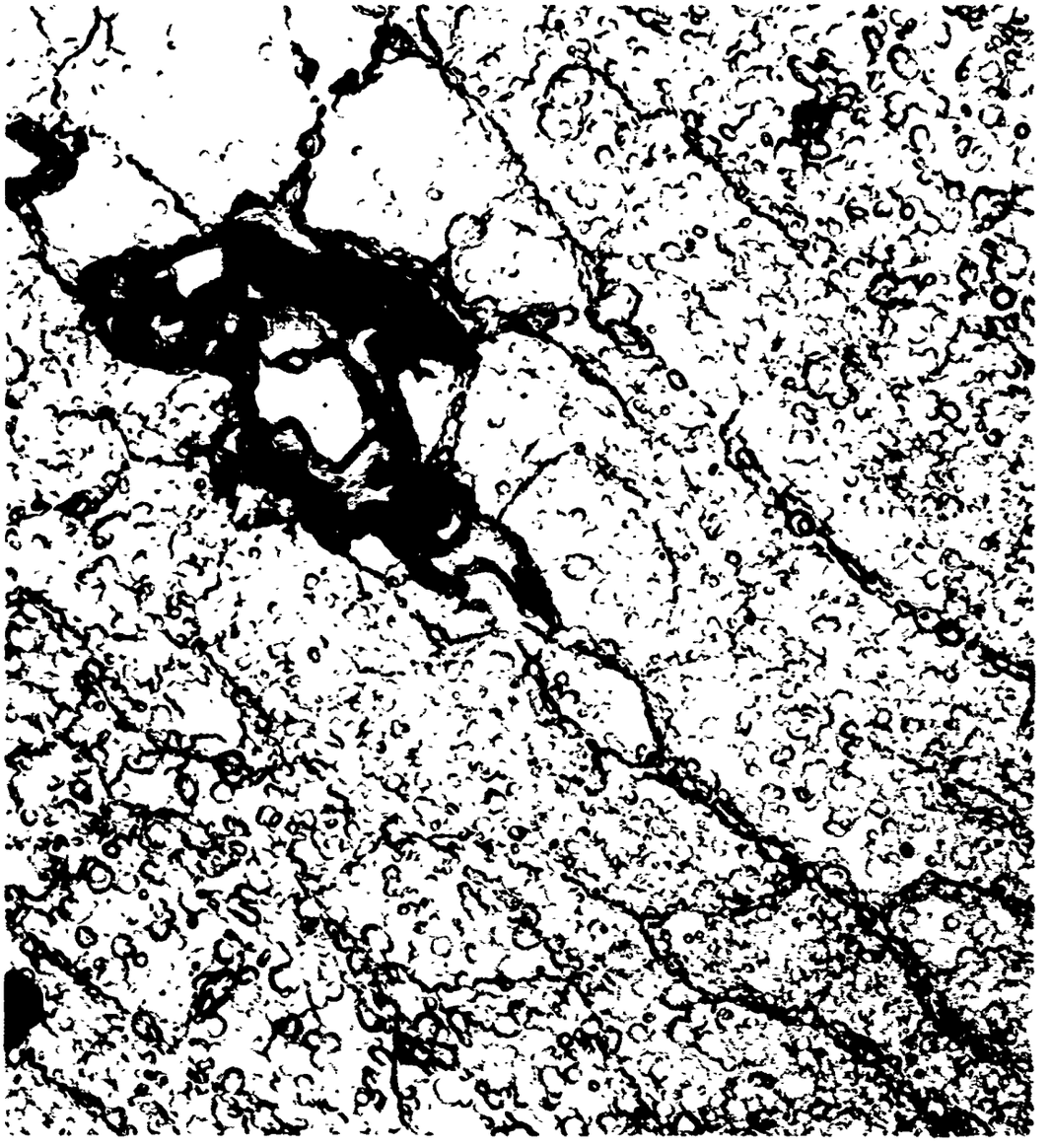

S-320832-E7A Neg. 153/9/5 10,000X

7075-T73 Stressed 75%Y.S. -0.950 V/18 Hrs.

**Figure 33**

Figure 34

Oxide replica of a prepolished specimen of 7075-T73 alloy plate exposed stressed at -1.150 volts for 18 hours. Large pits were not actually found in this particular replica, nevertheless, the attack appears quite similar to that in Figure 29.

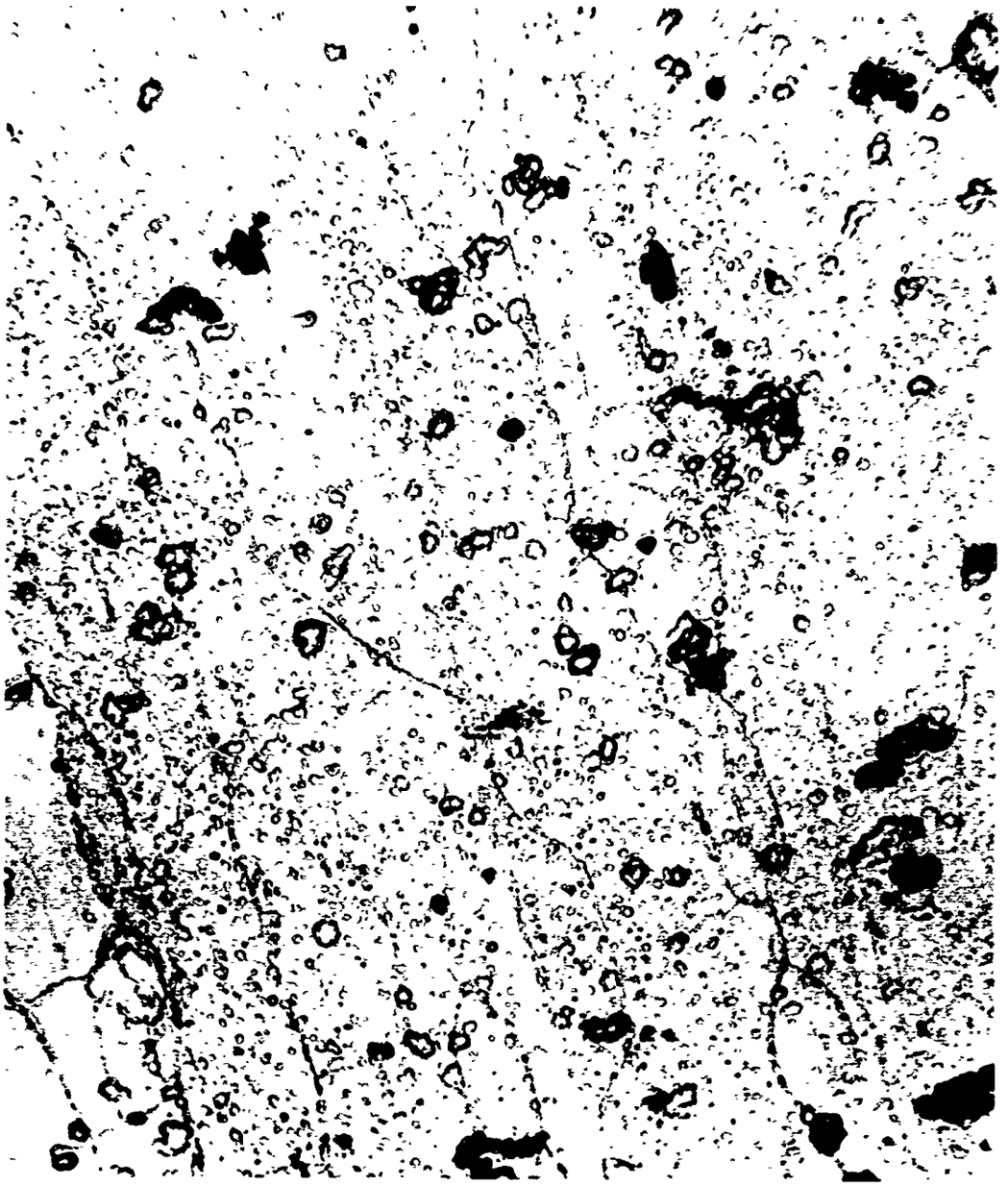

S-320832-E6A Neg. 151/12/6 5,000X

7075-T73 Stressed 75%Y.S. -1.150 V/18 Hrs.

**Figure 34**

Figure 35

Oxide replica of a prepolished specimen of 7075-T73 alloy plate exposed stressed at -1.250 volts for 18 hours. Cubic type pits are very much in evidence.

S-320832-E11A Neg. 152/13/6 5,000X

7075-T73 Stressed 75%Y.S. -1.250 V/18 Hrs.

**Figure 35**

Figure 36

Oxide replica of a prepolished specimen of 7075-T73 alloy plate exposed stressed at -1.325 volts for 18 hours. A number of tiny cubic pits were in evidence, but the matrix attack was very slight and resembled that in other specimens exposed at -1.320 to -1.350 volts.

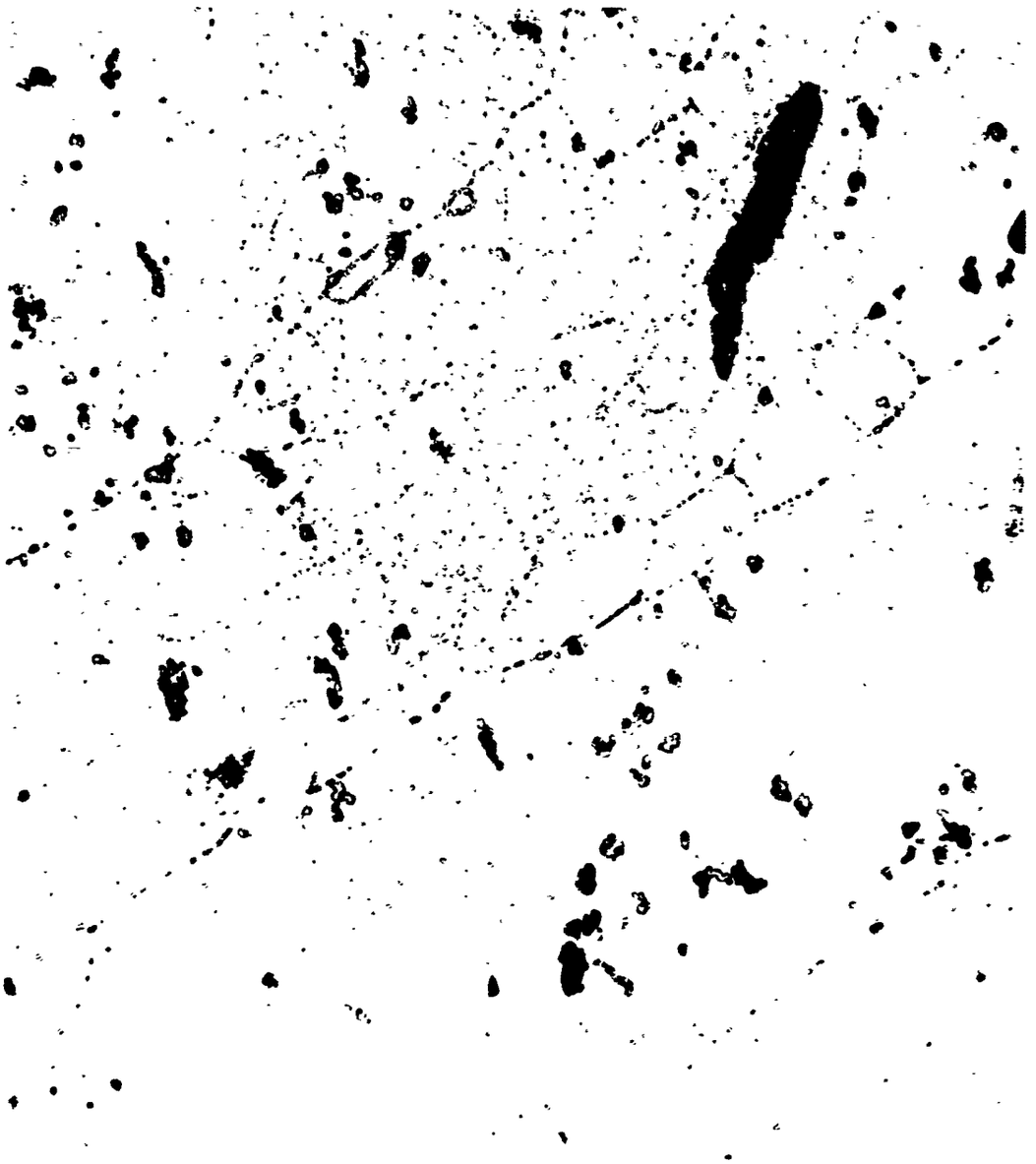

S-320832-E8A Neg. 151/13/3 5,000X

7075-T73 Stressed 75% Y. S. -1.325 V/18 Hrs.

Figure 36

Figure 37

Oxide replica of a prepolished specimen of high purity 7075-T6 alloy forging exposed stressed at -1.150 volts for 48 hours. The intergranular crack in the figure appeared to be associated with a small corrosion pit, but there was no evidence of any constituent particles near the crack. The long exposure produced a "pebbled" appearance - possibly by the mechanical action of hydrogen bubbles streaming upwards.

S-321854-E1 Neg. 153/6/1 5,000X

H.P. 7075-T6 Forging Stressed 75%Y.S. -1.150 V/48 Hrs.

Figure 37

Figure 38

Oxide replica of a prepolished specimen of high purity 7075-T6 alloy forging exposed stressed at -1.150 volts for 72 hours. As in Figure 37, a crack was seen which may have been associated with a corrosion pit, but not with constituent particles. The pebbled appearance was even more severe than in Figure 37. Exposures were attempted for longer periods, but the pebbled appearance completely obliterated any other effect.

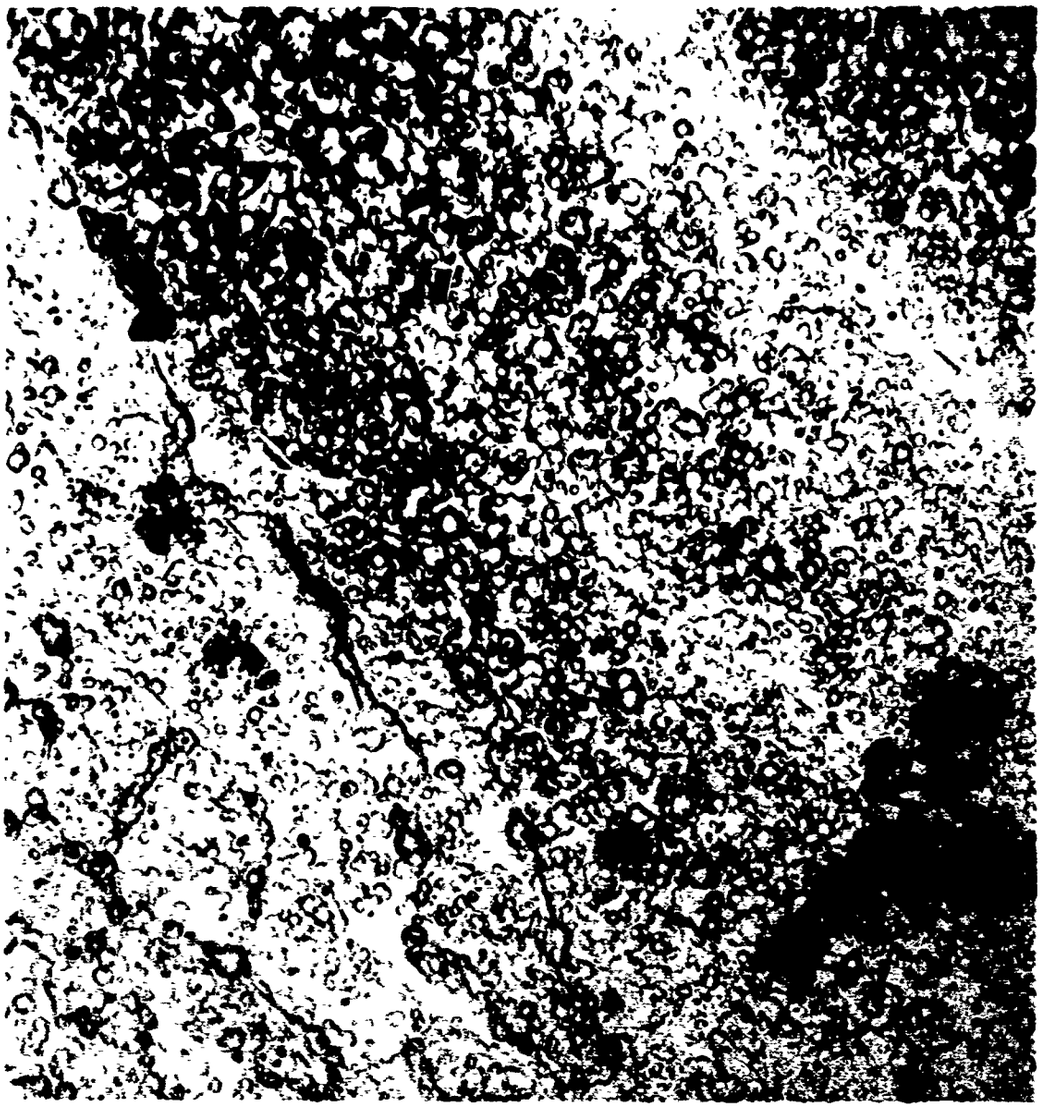

S-321854-E2 Neg. 153/6/4 5,000X

H.P. 7075-T6 Forging Stressed 75%Y.S. -1.150 V/72 Hrs.

Figure 38

Figure 39

Correlation between resistance change and crack depth for tensile specimens of 7075-T6 alloy exposed at stresses ranging from 50% to 90%Y.S. and at a variety of potentials. As illustrated, crack depth was taken as the width of the bright, intergranular region of the fracture surface; it was measured microscopically. Resistance change at failure was obtained by extrapolation of the resistance-time curve.

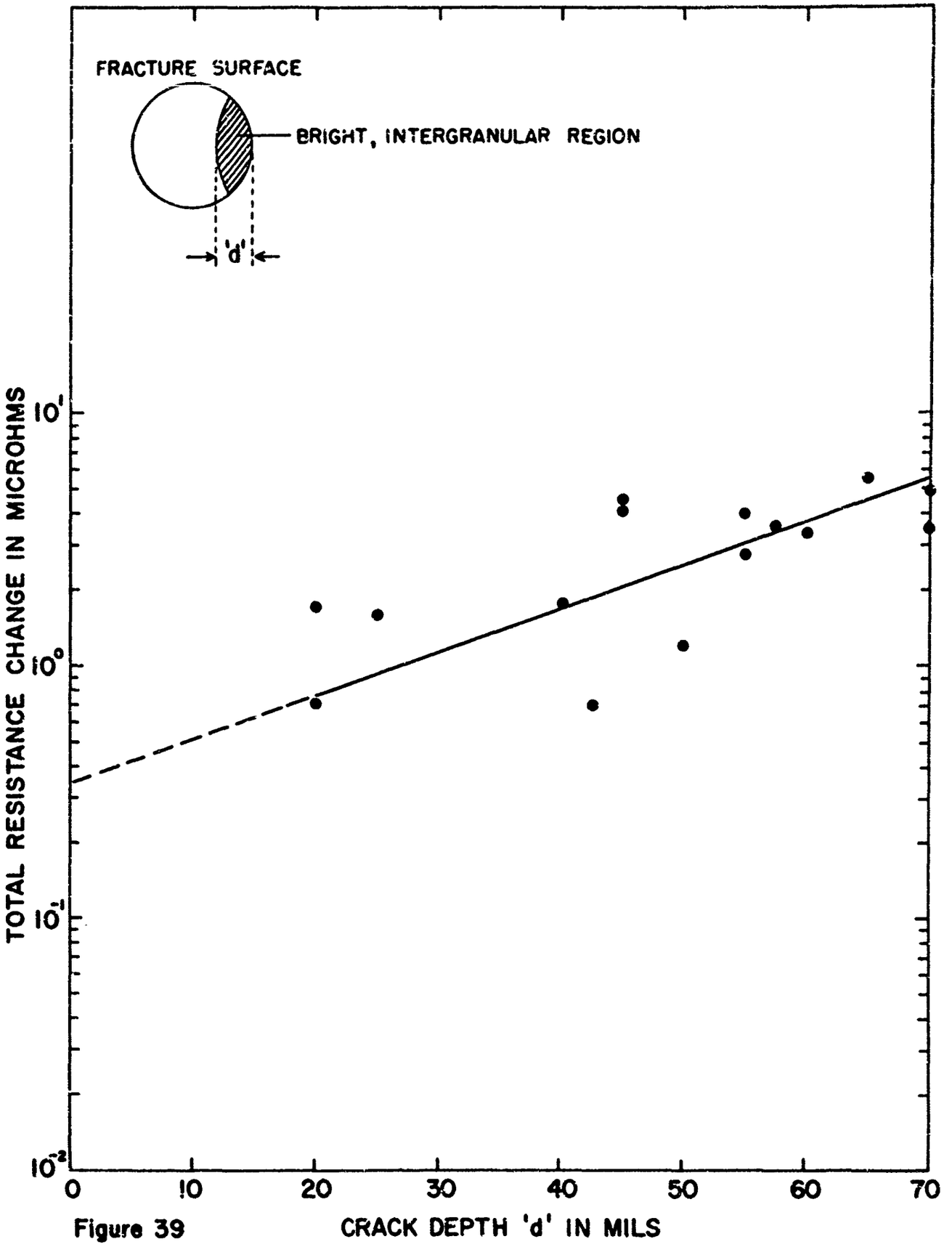
FRACTURE SURFACE
BRIGHT, INTERGRANULAR REGION
'd'
TOTAL RESISTANCE CHANGE IN MICROHMS
$10^{1}$
$10^{0}$
$10^{-1}$
$10^{-2}$
0
10
20
30
40
50
60
70
CRACK DEPTH 'd' IN MILS

Figure 39

Figure 40

Correlation between resistance change and per cent loss in tensile strength for specimens of 7075-T6 alloy. Stressed (75%Y.S.) specimens were exposed at free corrosion and -1.150 volts; unstressed specimens were exposed at free corrosion only. An exposure was continued until a measurable resistance change had occurred; the specimen was then removed and tensile tested, in some cases stressed specimens were allowed to proceed to failure. The loss in tensile strength was calculated for these specimens by assuming that the final strength equaled 75% of the initial yield strength.

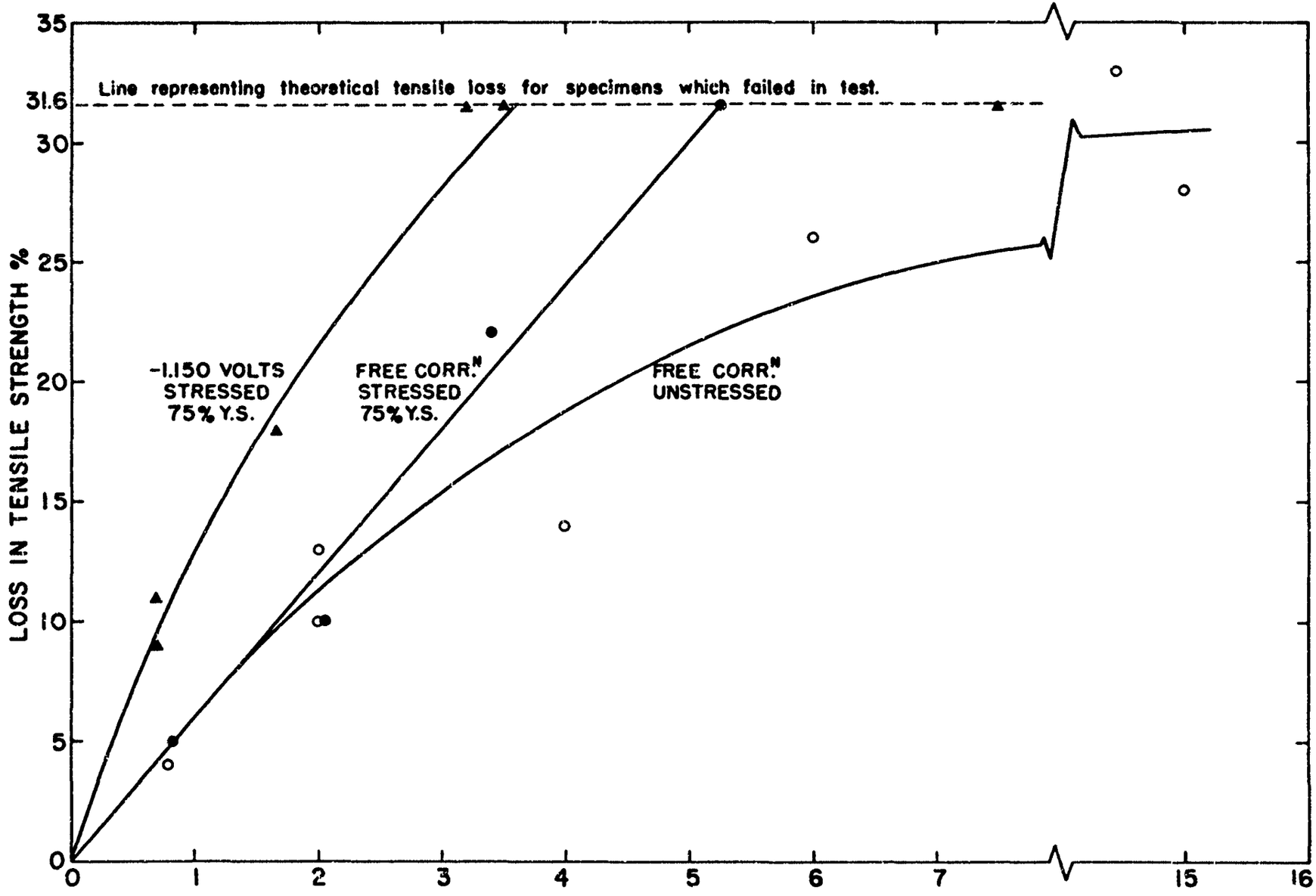
35
31.6
30
25
20
15
10
5
0
Line representing theoretical tensile loss for specimens which failed in test.
-1.150 VOLTS
STRESSED
75% Y.S.
FREE CORR.N
STRESSED
75% Y.S.
FREE CORR.N
UNSTRESSED
LOSS IN TENSILE STRENGTH %
0
1
2
3
4
5
6
7
15
16
RESISTANCE CHANGE IN MICROHMS

Figure 40

Figure 41

The effect of potential on the third stage of the resistance vs. time curve for tensile specimens of two alloys failing by stress corrosion. Each specimen was exposed (stressed to 75%Y.S.) at various potentials, and the logarithmic slope of the third stage of the resistance vs. time curve was measured. The curves approach a zero value for $\frac{d \log \Delta R}{dt}$ at discrete potentials of approximately -1.3 and -1.4 volts, respectively. These potentials appear to coincide with the respective protection potentials for the two alloys.

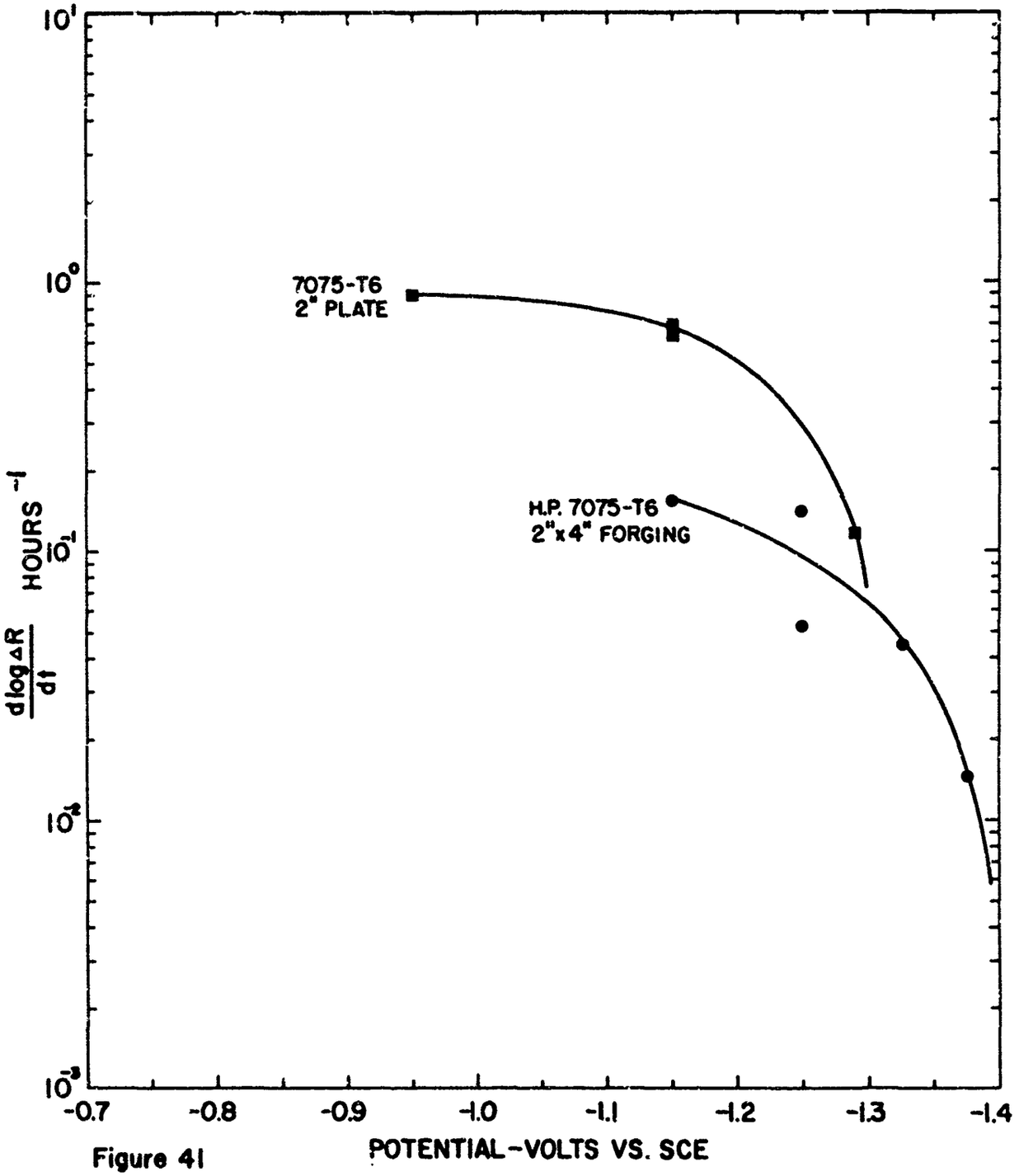
7075-T6
2" PLATE
H.P. 7075-T6
2"x4" FORGING
$\frac{d \log \Delta R}{dt}$ HOURS$^{-1}$
$10^{1}$
$10^{0}$
$10^{-1}$
$10^{-2}$
$10^{-3}$
-0.7
-0.8
-0.9
-1.0
-1.1
-1.2
-1.3
-1.4
POTENTIAL-VOLTS VS. SCE

Figure 41

# Appendix A

## Calculation of Correction for IR Drop

At the current densities encountered in the cathodic protection experiments, it was necessary to apply a correction for the IR drop in the solution between the tip of the Luggin capillary and the specimen. Considering the IR drop to be positive in sign and the measured potential $E_m$ to be negative in sign, the corrected potential of the cathode $E_c$ is:

$$E_c = E_m + (IR) \qquad (1)$$

$E_m$ is equal in magnitude to the control potential setting on the potentiostat; therefore, it is evident that the control potential setting must vary with the current density if $E_c$ is to be constant. This adjustment was made manually as required.

In order to calculate the appropriate correction, it was necessary to know the value of R; this value was determined separately for each of the two types of specimen employed.

Tensile Specimens - By means of a movable capillary, it was found that the potential distribution followed the ideal law for concentric cylinders for distances up to about 1 centimeter from the surface of the specimen. The resistance could be calculated from the following equation:

$$R = \frac{\rho}{2\pi} \ln (r_2/r_1) \qquad (2)$$

where $\rho$ is the resistivity of the solution (7.86 ohm-cm at 25°C), $r_1$ is the radius of the specimen in centimeters, $r_2$ is the

corresponding radius out to the tip of the Luggin capillary and R is the resistance of an annular cylinder of solution surrounding the specimen and having the following dimensions: height of 1 centimeter, inner diameter of $2r_1$ and outer diameter of $2r_2$. The correction to the measured potential is then the product I x R, where R is given by equation (1) and I is the current flowing to the corresponding area. Expressed in terms of the current density i the correction is:

$$IR = (i\ 2\pi r_1)\ \frac{\rho}{2\pi}\ \ln (r_2/r_1) = ir_1\rho \ln (r_2/r_1) \qquad (3)$$

For a 3 millimeter spacing, equation (3) becomes:

$$IR = 1.32\ i \qquad (4)$$

Sheet Specimens - An unstressed, polished specimen of 7075-T6 alloy was mounted in the normal way, and held at a constant potential versus a fixed Luggin capillary. A second capillary was moved in and out along a line perpendicular to the center of the specimen, and the measured potential was plotted against the distance from the specimen. For this experiment, a Leeds and Northrup Type K3 potentiometer was used to measure potentials.

The results are shown in Figure 42. Figure 43 is a plot of the slope of the curve in Figure 42 as a function of the abscissa. (The slopes were measured geometrically.) The horizontal part of the plot is not derived from Figure 42; it corresponds to the limiting case of an infinite plane specimen for which the relationship

$$R = \rho\frac{x}{A} \qquad (5)$$

applies. The value of R in this case is a linear function of x, and the slope of x vs $E_m$ is independent of x. The value of this slope was calculated as follows:

$$dE_m = -idR \quad \text{from (1)}$$

From (5)

$$dR = \frac{\rho dx}{A}$$

$$\therefore \quad dE_m = \frac{-i\rho dx}{A}$$

or

$$\frac{dx}{dE_m} = \frac{-A}{i\rho}$$

Inserting the experimental values: $A = 2$ sq. cms

$i = 27$ mA

$\rho = 7.86$ ohm cms

gives $\frac{dx}{dE_m} = -94.2$ mm/volt

and this equation corresponds to the horizontal line in Figure 43.

To extrapolate the experimental line below the point of intersection with the horizontal line is not justified since it would imply that the IR drop in this region was greater than for a linear potential gradient, and this is highly unlikely.

The resistance between the specimen and a point at any distance x (up to about 5 mm) is calculated as follows:

$$R = R_o^a + R_a^x$$

Where $R_o^a$ is the resistance from o to a*, - calculated from equation (5) - and $R_a^x$ is the resistance from a to x, which is calculated empirically as follows:

From Figure 43,

$$\frac{dx}{dE} = 43.2x + 36 \quad \text{(up to } x = 5 \text{ mm)} \qquad (6)$$

$$\therefore \quad \int_{E_a}^{E_x} -dE = \int_{a}^{x} \frac{dx}{43.2x + 36}$$

$$\therefore \quad E_a - E_x = \frac{1}{43.2} \ln \frac{(43.2x + 36)}{(42.2a + 36)}$$

For $x = 3$ mm, which is the distance used in the actual tests:

$$E_a - E_x = 0.0130 \text{ V} = IR_a^x$$

$$\therefore \quad R_a^x = \frac{0.0130}{0.027} \quad \text{since } i = 27 \text{ mA in this experiment}$$

$$= 0.48 \text{ ohms}$$

$$\text{and} \quad R_o^a = 0.53 \text{ ohms from equation (5)}$$

$$\therefore \quad R = 1.01 \text{ ohms}$$

(*a is the value of x at which the two straight lines intersect, and was taken as 1.35 mm.)

It is recognized that this calculation of R is only approximate, since the exact form of the curve of $E_m$ vs x is not known close to the specimen. However, the error is likely to be only a few per cent, and would be too small to have a serious effect on the corrected potential. For example, the true potential for the specimen used in this experiment would be:

$$E_c = E_m + IR$$

$$= -1.328 + (27 \cdot 10^{-3} \cdot 1.01) \text{ volts} \quad (E_m = -1.328 \text{ V from Figure 42})$$

$$= -1.301 \text{ volts}$$

and an error of 5% in R would produce an error of only 0.001 volts in $E_c$.

Figure 42

Curve of measured potential versus distance between the specimen and the Luggin capillary tip. The data were obtained as follows: A prepolished specimen of 7075-T6 alloy plate was exposed unstressed at a potential of about -1.340 volts vs a fixed Luggin capillary. A movable Luggin capillary was then used to determine the apparent potential as a function of distance from the specimen - along the normal to the middle of the specimen. The open symbols represent readings moving away, and the closed symbols represent readings moving back towards the specimen.

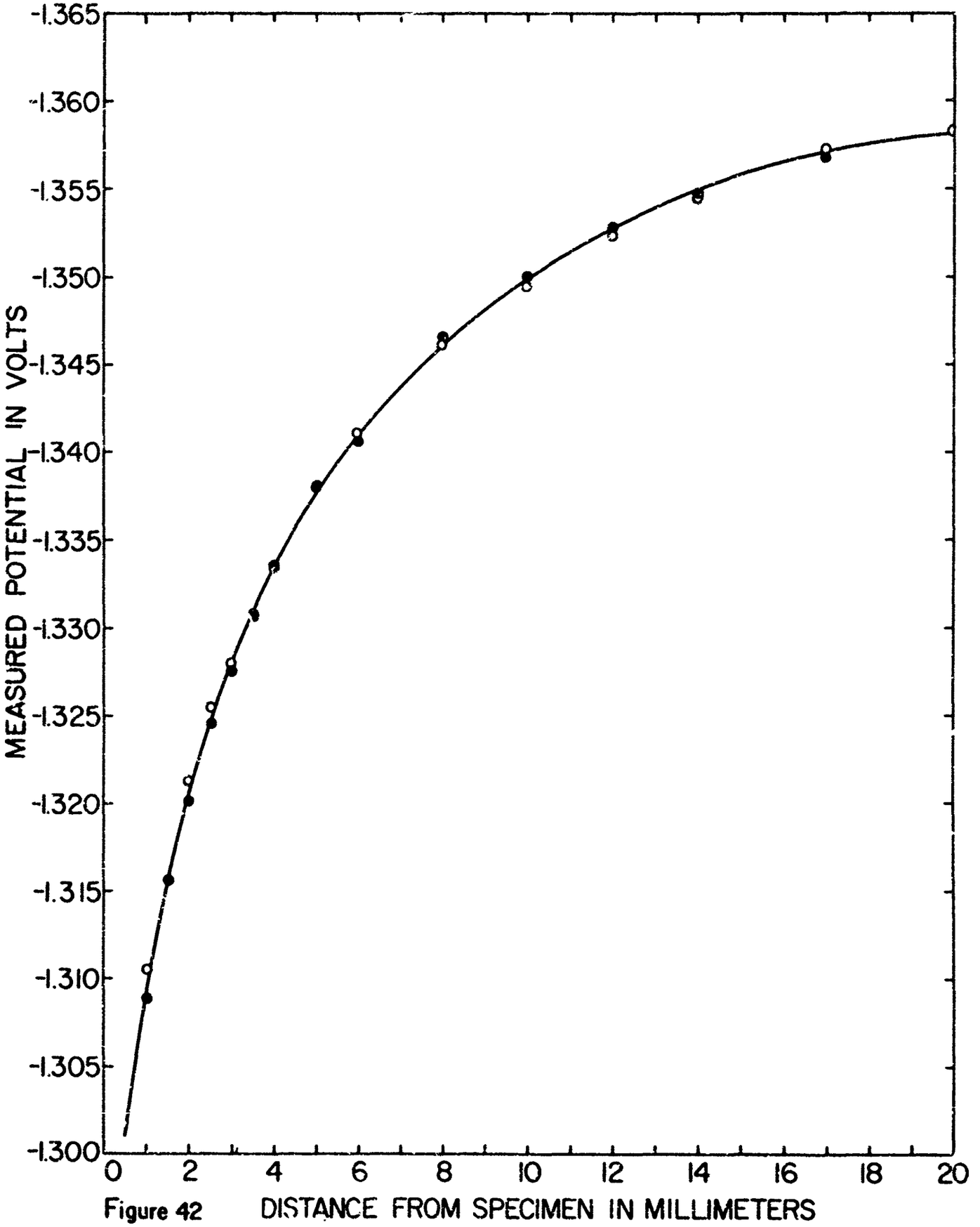
-1.365
-1.360
-1.355
-1.350
-1.345
-1.340
-1.335
-1.330
-1.325
-1.320
-1.315
-1.310
-1.305
-1.300
MEASURED POTENTIAL IN VOLTS
0
2
4
6
8
10
12
14
16
18
20
DISTANCE FROM SPECIMEN IN MILLIMETERS

Figure 42

Figure 43

Curve of the reciprocal of measured potential gradient versus distance from the specimen. The data was obtained from Figure 42 by graphical measurements of the slope at various points on the curve. The horizontal line at 94.2 millimeters/volt corresponds to the limiting situation of an infinite plane specimen, where the current flow in the solution is normal to the surface of the specimen. The intersection of the horizontal line with the experimental curve corresponded to a distance of 1.35 millimeters - designated "a" on the figure.

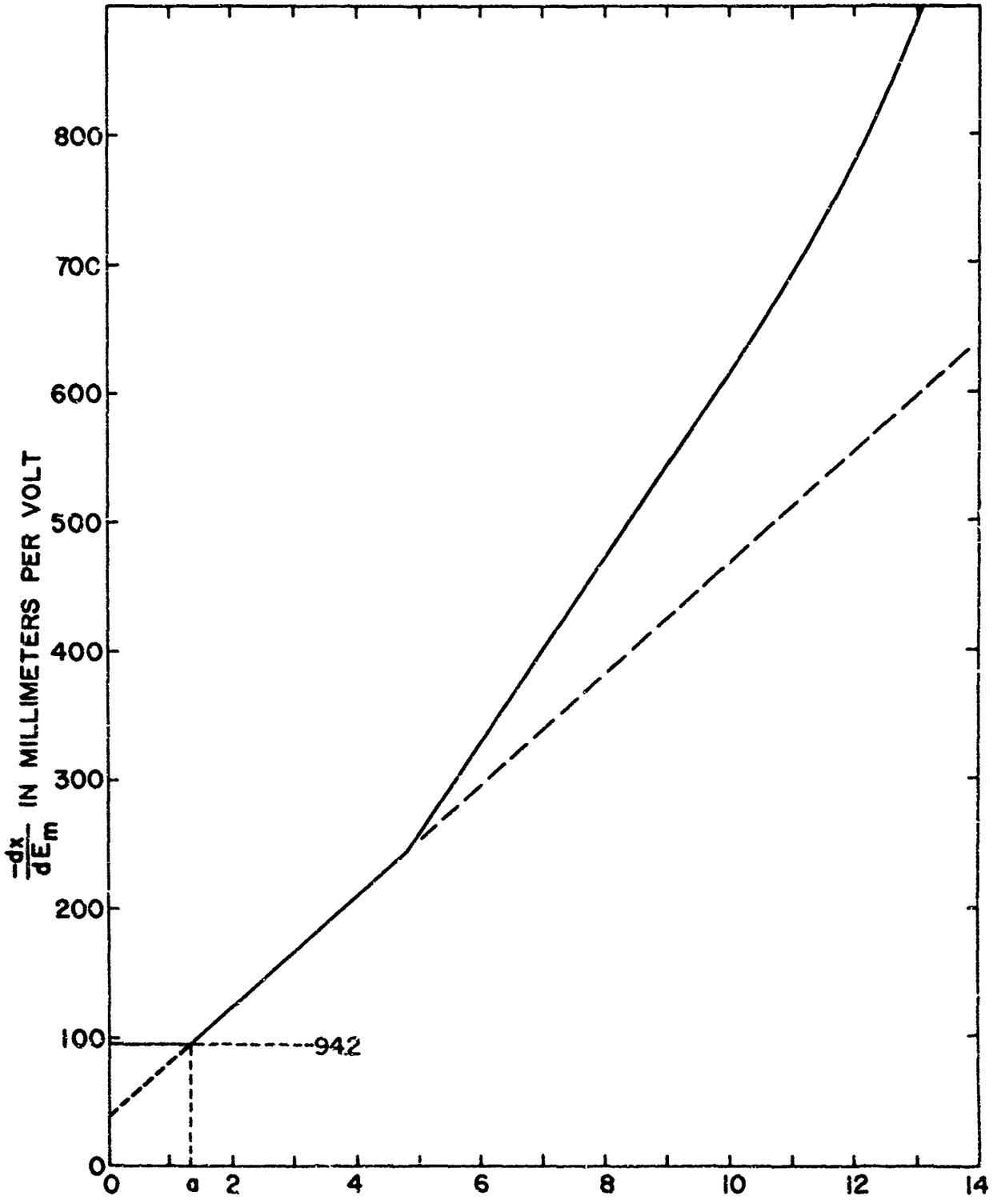


Figure 43 DISTANCE FROM SPECIMEN IN MILLIMETERS

## Appendix B

## Correlation Between Resistance Change and Crack Depth

Figure 39 indicates a relationship between resistance change ($\Delta R$) and crack depth (d) of the form

$$57.8 \log \Delta R = d + 27 \qquad (1)$$

In one experiment, a plot was obtained of $\Delta R$ vs time for a stressed specimen of 7075-T6 exposed at 0.950 volts. The slope of the exponential stage on semi-logarithmic axes was:

$$\frac{d\ (\log \Delta R)}{dt} = 0.9 \text{ hours}^{-1} \qquad (2)$$

Differentiating (1)

$$57.8 \frac{(d \log \Delta R)}{dt} = \frac{dd}{dt}$$

Substituting from (2)

$$\therefore \quad \frac{dd}{dt} = 0.9 \times 57.8 \cdot 10^{-3} \text{ inches/hour}$$

$$= 0.05 \text{ inches/hour}$$

## Appendix C

## Calculation of the Anodic Current Density Necessary to Account for Stress-Corrosion Cracking

Let Total anodic current = I amps

Area of tip of crack = A sq cms

Crack propagation rate = V cms/sec.

Density of metal = D gms/ml (2.7 gms/ml for aluminum)

Volume of metal dissolved = VA ml/sec.

Weight of metal dissolved = VAD ml/sec.

Faradaic current equivalent I = $\frac{2.7\ VA}{9}$ x 96,500 amps (for aluminum)

Anodic current density $\frac{I}{A}$ = $\frac{2.7 \times 96,500}{9}$ V amps/sq cm

= 30,000 V amps/sq cm approximately

Thus for the crack propagation rate of 0.05 inches/hour (i.e., $3.5 \times 10^{-5}$ cms/second) calculated for a 7075-T6 specimen at -0.950 volts vs S.C.E., the anodic current density at the tip of the crack would have to be approximately 1 amp per square centimeter.